

Flux-corrected transport stabilization of an evolutionary cross-diffusion cancer invasion model

Shahin Heydari ^{*1}, Petr Knobloch ^{†1}, and Thomas Wick ^{‡2}

¹Charles University, Faculty of Mathematics and Physics, Sokolovská 83,
18675 Praha 8, Czech Republic

²Leibniz University Hannover, Institute of Applied Mathematics,
Welfengarten 1, 30167 Hannover, Germany

Abstract

In the present work, we investigate a model of the invasion of healthy tissue by cancer cells which is described by a system of nonlinear PDEs consisting of a cross-diffusion-reaction equation and two additional nonlinear ordinary differential equations. We show that when the convective part of the system, the chemotactic term, is dominant, then straightforward numerical methods for the studied system may be unstable. We present an implicit finite element method using conforming P_1 or Q_1 finite elements to discretize the model in space and the θ -method for discretization in time. The discrete problem is stabilized using a nonlinear flux-corrected transport approach. It is proved that both the nonlinear scheme and the linearized problems used in fixed-point iterations are solvable and positivity preserving. Several numerical experiments are presented in 2D using the deal.II library to demonstrate the performance of the proposed method.

Key words: cancer invasion, cross-diffusion equation, FEM-FCT stabilization, positivity preservation, existence of solutions

AMS Classification (2020): 65M22, 65M60, 92C17, 35Q92,

1 Introduction

Keller and Segel [29, 28] proposed the first mathematical model for description of chemotactical processes. Chemotaxis refers to the motion in the direction to (or away from) the position of higher concentration based on the gradient of chemical substances and its chemotacticity character which controls the speed of this motion. Their model has been widely extended and followed to develop more sophisticated and complex chemotaxis models and played a vitally important role in many areas of science, in particular in medical and biological applications, for example, bacteria and cell aggregation [1, 39, 51], tumor angiogenesis and invasion [3, 11, 12, 13], biological pattern formation [2, 51], and immune cell migration [54]. From the analytical point of view,

*e-mail: heydari@karlin.mff.cuni.cz , corresponding author

†e-mail: knobloch@karlin.mff.cuni.cz

‡e-mail: thomas.wick@ifam.uni-hannover.de

mathematical analysis for chemotaxis systems of equations is a challenge and causes many questions especially in the context of the existence and uniqueness of solutions. In the last three decades, many researchers have been actively involved and answered some of these questions [40, 16, 23, 49, 22, 10]. From the numerical point of view, so far a great deal of research on chemotaxis models has been done in various areas, including the finite difference method [11, 12, 31], discontinuous Galerkin method [18, 35], finite element method [43, 56, 57], finite volume method [20], operator-splitting methods [42], or fractional step algorithms [52]. However, many analytical and numerical aspects are still untouched and call for further investigation.

The chemotaxis problems are usually strongly coupled nonlinear systems of equations whose solutions represent concentrations or densities and need to be non-negative in order to satisfy the physics behind the system. Hence, it is difficult to construct an efficient and accurate numerical method that does not produce solutions with negative values. Another interesting aspect is singular, spiky and oscillatory behavior of the solutions. In particular, when the chemotaxis term dominates the diffusion and reaction terms, in other words large chemosensitivity is present which corresponds to large Reynolds numbers, it may give rise to nonphysical oscillations in the solution. To overcome this problem, stabilization methods can be applied. Up to now, many scientists used flux-corrected transport (FCT) algorithms, i.e., nonlinear high-resolution schemes introduced by Boris and Book [8, 7, 9], later developed based on linear finite element discretizations by Kuzmin, Löhner et al. [36, 33, 34, 32], and further extended to linear and nonlinear space-time FEM-FCT in [19]. In [46], an implicit flux-corrected transport scheme was developed and applied to three benchmark examples of the general Keller–Segal model in two spatial dimensions. It was shown that the proposed method is positivity preserving and sufficiently accurate, even in the cases where solutions blow up in the center or at the boundary of the domain. The investigations of the blow-up behavior of the solutions were further extended to three spatial dimensions in [47]. In [45, 44], an FEM-FCT scheme was coupled with a level-set method to obtain positivity preserving solutions on a stationary surface and evolving-in-time surfaces. It was shown that the proposed method is able to produce accurate numerical solutions, which makes it possible to couple the partial differential equations defined on a specific domain with the PDEs that are defined on the surface of this domain. This scheme was further used with operator-splitting techniques to solve chemotaxis models in 3D. The operator-splitting method splitted a 3D problem into a sequence of 1D subproblems and the FEM-FCT algorithm was used to solve each 1D subproblem separately [25]. In [48], the authors used an efficient adaptive moving mesh finite element approach based on the parabolic Monge–Ampère method for determining the coordinate transformation for the adaptive mesh combined with an FCT scheme which guarantees the non-negativity of the solutions. As a result, the computational cost was significantly reduced. All aforementioned techniques were also applied to the same benchmark examples. A different case was studied in [24], where the authors used the pressure-correction scheme and flux-corrected transport algorithm to propose an efficient linear positivity-preserving method for the solution of chemotaxis–Stokes equations.

In this work, we focus on a cancer-invasion model developed in [41], modeling the motion of cancer cells, degradation of extracellular matrix, and certain enzymes (e.g., protease). The extracellular matrix is degraded upon contact with protease which is produced where cancer cells and extracellular matrix meet and decay over the time. In [21], we extended the proposed model by a diffusion term, gave a rigorous proof for the existence of the global classical solution and presented numerical results for a Galerkin finite element discretization. In the present paper, a diffusion term is not considered, which makes the problem more challenging. In [30], one of the authors of the present paper applied a positivity preserving non-standard finite difference method to solve the nonlinear system in 1D, see also [14] for related approaches. Here, we consider the finite element method and apply the FCT technique to guarantee the positivity preservation. First, however, we consider the more diffusive nonlinear low-order method. An additional nonlinearity is then introduced by the flux correction. We prove that both nonlinear problems are solvable and positivity preserving. To the best of our knowledge, the current work is a first attempt to gain an insight into the applicability of the FCT technique to the numerical solution of a chemotaxis system without self-diffusion and to provide a rigorous analysis of the solvability and positivity preservation. Note that the existence and uniqueness for the FEM-FCT method applied to linear

evolutionary convection-diffusion equations has been addressed only recently in [27, 26]. We also present a fixed-point algorithm for the iterative solution of the FCT discretization and prove that it is well posed and provides a non-negative solution at each step. Consequently, the non-negativity of the approximate solution is guaranteed independently of the choice of a stopping criterion. The properties of the proposed FCT scheme are illustrated by various numerical simulations carried out using our newly designed algorithm in the deal.II library [4, 5].

The outline of this paper is as follows. In Section 2, we formulate the mathematical model which is discretized by the Galerkin method in Section 3. Then, the FCT stabilization is introduced in Section 4, where also the solvability and positivity preservation is proved. The fixed-point algorithm is proposed and investigated in Section 5. In Section 6, we report several numerical simulations in two spatial dimensions carried out for various regimes. Finally, our results are summarized in Section 7.

2 Mathematical model

In this section, we discuss the following nondimensionalized continuous model of a malignant cancer invasion proposed by Perumpanani et al. in [41, 37]. The model contains three unknown variables, namely the cancer cell density $u = u(x, t)$, connective tissue $c = c(x, t)$, and protease $p = p(x, t)$, and it consists of the equations

$$\frac{\partial u}{\partial t} = \mu u(1 - u) - \chi \nabla \cdot (u \nabla c) \quad \text{in } \Omega \times (0, T], \quad (2.1)$$

$$\frac{\partial c}{\partial t} = -pc \quad \text{in } \Omega \times (0, T], \quad (2.2)$$

$$\frac{\partial p}{\partial t} = \epsilon^{-1}(uc - p) \quad \text{in } \Omega \times (0, T], \quad (2.3)$$

where Ω is a bounded polyhedral domain in \mathbb{R}^d , $d \in \{1, 2, 3\}$, $[0, T]$ is a time interval, and μ, χ, ϵ are positive constants. Here, μ and χ denote the proliferation and haptotaxis rate of cancer cells, respectively, and the parameter ϵ is supposed to be small since the units of connective tissues and invasive cells are much larger than the protease. In the process of invasion, the connective tissue is affected by the invasive flux of $u \nabla c$ into its compartment. Since the connective tissue does not contain any empty space large enough for passing of passive cancer cells, it degrades by protease which is produced by invasive cancer cells upon contact with connective tissue. It can be shown that if the initial conditions of the above model are non-negative, then the computed solutions stay non-negative at all times, for more details see [37, 38, 14] and the references therein.

The system (2.1)–(2.3) is subjected to the homogeneous Neumann boundary condition

$$u \frac{\partial c}{\partial n} = 0 \quad \text{on } \partial\Omega \times [0, T], \quad (2.4)$$

where n is the unit outward normal vector on $\partial\Omega$. The above equations are endowed with the initial conditions

$$u(x, 0) = u^0(x), \quad c(x, 0) = c^0(x), \quad p(x, 0) = p^0(x), \quad x \in \Omega, \quad (2.5)$$

where $u^0, c^0, p^0 : \Omega \rightarrow [0, 1]$ are given functions.

In [21], we considered a modified version of (2.1)–(2.3) containing an extra diffusion term in (2.1). Precisely, instead of the equation (2.1), we considered

$$\frac{\partial u}{\partial t} = \mu u(1 - u) - \chi \nabla \cdot (u \nabla c) + \alpha^{-1} \Delta u \quad \text{in } \Omega \times (0, T] \quad (2.6)$$

with a positive constant α . This required to replace the boundary condition (2.4) by

$$\alpha^{-1} \frac{\partial u}{\partial n} = \chi u \frac{\partial c}{\partial n} \quad \text{on } \partial\Omega \times [0, T].$$

Thus, the problem considered in this paper corresponds to the limit case $\alpha \rightarrow \infty$ of the problem from [21]. In that paper, we proved the existence of global classical solutions for two- and three-dimensional bounded domains Ω with smooth boundaries and we proved that these solutions are non-negative. Moreover, we showed that by fixing the proliferation rate μ and varying the haptotaxis χ one can make either the diffusion or the transport of the cancer cells dominant. The domination of the convection term can produce spurious oscillations and a blow-up in the solution of the system as it is the case to be considered in here.

3 A Galerkin discretization

The solution of the problem (2.1)–(2.5) satisfies

$$\left(\frac{\partial u}{\partial t}, v \right) = \mu (u(1-u), v) + \chi (u \nabla c, \nabla v) \quad \text{in } (0, T] \text{ and for } v \in H^1(\Omega), \quad (3.1)$$

$$c(x, t) = c^0(x) e^{-\int_0^t p(x, s) ds} \quad \forall (x, t) \in \Omega \times [0, T], \quad (3.2)$$

$$p(x, t) = e^{-t/\epsilon} \left[p^0(x) + \frac{1}{\epsilon} \int_0^t u(x, s) c(x, s) e^{s/\epsilon} ds \right] \quad \forall (x, t) \in \Omega \times [0, T], \quad (3.3)$$

where (\cdot, \cdot) denotes the inner product in $L^2(\Omega)$ or $L^2(\Omega)^d$. To define an approximate solution of (2.1)–(2.5), we first introduce a triangulation \mathcal{T}_h of Ω consisting of simplicial (for $d = 1, 2, 3$), quadrilateral (for $d = 2$) or hexahedral (for $d = 3$) shape-regular cells possessing the usual compatibility properties (see, e.g., [15]). For any cell $K \in \mathcal{T}_h$, we denote by h_K the diameter of K and assume that $h_K \leq h$. We denote by $V_h \subset H^1(\Omega)$ the usual conforming P_1 or Q_1 finite element space constructed using the triangulation \mathcal{T}_h . Let ϕ_1, \dots, ϕ_M be the standard basis functions of V_h associated with the vertices x_1, \dots, x_M of \mathcal{T}_h . Thus, the basis functions are non-negative and satisfy $\phi_i(x_j) = \delta_{ij}$ for $i, j = 1, \dots, M$, where δ_{ij} is the Kronecker symbol. Any function $v_h \in V_h$ can be identified with a coefficient vector $\mathbf{v} = (v_j)_{j=1}^M$ with respect to these basis functions. Precisely, introducing the bijective operator $\pi_h : \mathbb{R}^M \rightarrow V_h$ by

$$\pi_h \mathbf{v} = \sum_{j=1}^M v_j \phi_j,$$

one has $v_h = \pi_h \mathbf{v}$. The assumed shape regularity of \mathcal{T}_h implies that

$$\|\nabla \phi_i\|_{L^2(K)} \leq \kappa h_K^{d/2-1} \quad \forall K \in \mathcal{T}_h, i = 1, \dots, M, \quad (3.4)$$

where κ is a fixed constant independent of i , K , and h . Next, the time interval $[0, T]$ is decomposed by $0 = t_0 < t_1 < \dots < t_N = T$ and we set $\tau_n = t_n - t_{n-1}$, $n = 1, \dots, N$. At each time level t_n , the solution of (2.1)–(2.5) will be approximated by functions $u_h^n, c_h^n, p_h^n \in V_h$. These functions can be identified with coefficient vectors $\mathbf{u}^n = (u_j^n)_{j=1}^M$, $\mathbf{c}^n = (c_j^n)_{j=1}^M$, $\mathbf{p}^n = (p_j^n)_{j=1}^M$, respectively, satisfying $u_h^n = \pi_h \mathbf{u}^n$, $c_h^n = \pi_h \mathbf{c}^n$, $p_h^n = \pi_h \mathbf{p}^n$. Note that $u_h^n(x_i) = u_i^n$, $c_h^n(x_i) = c_i^n$, and $p_h^n(x_i) = p_i^n$ for $i = 1, \dots, M$. We set

$$u_i^0 = u^0(x_i), \quad c_i^0 = c^0(x_i), \quad p_i^0 = p^0(x_i), \quad i = 1, \dots, M. \quad (3.5)$$

Using linear interpolation with respect to time between the time levels gives functions $u_{h,\tau}, c_{h,\tau}, p_{h,\tau}$ defined on $\bar{\Omega} \times [0, T]$. For example, $u_{h,\tau}$ satisfies

$$u_{h,\tau}(x, t) = \frac{1}{\tau_{n+1}} [u_h^{n+1}(x)(t - t_n) + u_h^n(x)(t_{n+1} - t)] \quad \forall x \in \bar{\Omega}, t \in [t_n, t_{n+1}], n = 0, \dots, N-1,$$

or, equivalently,

$$u_{h,\tau}(x_i, t) = \frac{1}{\tau_{n+1}} [u_i^{n+1}(t - t_n) + u_i^n(t_{n+1} - t)] \quad \forall i = 1, \dots, M, \quad t \in [t_n, t_{n+1}], \quad n = 0, \dots, N-1.$$

Replacing the space $H^1(\Omega)$ in (3.1) by V_h and applying the θ -method for discretization in time (with $\theta \in [0, 1]$), one obtains

$$\begin{aligned} \left(\frac{u_h^{n+1} - u_h^n}{\tau_{n+1}}, v_h \right) &= \theta \mu(u_h^{n+1}(1 - u_h^{n+1}), v_h) + \theta \chi(u_h^{n+1} \nabla c_h^{n+1}, \nabla v_h) \\ &+ (1 - \theta) \mu(u_h^n(1 - u_h^n), v_h) + (1 - \theta) \chi(u_h^n \nabla c_h^n, \nabla v_h) \quad \forall v_h \in V_h, \quad n = 0, \dots, N-1. \end{aligned} \quad (3.6)$$

Defining the matrices $\mathbb{M} = (m_{ij})_{i,j=1}^M$ and $\mathbb{A}^n = (a_{ij}^n)_{i,j=1}^M$ with

$$m_{ij} = (\phi_j, \phi_i), \quad a_{ij}^n = -\mu(\phi_j(1 - u_h^n), \phi_i) - \chi(\phi_j \nabla c_h^n, \nabla \phi_i),$$

the discrete variational problem (3.6) can be written in the matrix form

$$(\mathbb{M} + \theta \tau_{n+1} \mathbb{A}^{n+1}) \mathbf{u}^{n+1} = (\mathbb{M} - (1 - \theta) \tau_{n+1} \mathbb{A}^n) \mathbf{u}^n, \quad n = 0, \dots, N-1. \quad (3.7)$$

The relations (3.2) and (3.3) suggest to define the coefficients of c_h^n and p_h^n by

$$c_i^n = c^0(x_i) e^{-\int_0^{t_n} p_{h,\tau}(x_i, s) ds}, \quad i = 1, \dots, M, \quad n = 0, \dots, N, \quad (3.8)$$

$$p_i^n = e^{-t_n/\epsilon} \left[p^0(x_i) + \frac{1}{\epsilon} \int_0^{t_n} u_{h,\tau}(x_i, s) c_{h,\tau}(x_i, s) e^{s/\epsilon} ds \right], \quad i = 1, \dots, M, \quad n = 0, \dots, N. \quad (3.9)$$

Then, for $i = 1, \dots, M$ and $n = 0, \dots, N-1$, one has

$$c_i^{n+1} = c_i^n e^{-\int_{t_n}^{t_{n+1}} p_{h,\tau}(x_i, s) ds}, \quad (3.10)$$

$$p_i^{n+1} = e^{-\tau_{n+1}/\epsilon} p_i^n + \frac{1}{\epsilon} e^{-t_{n+1}/\epsilon} \int_{t_n}^{t_{n+1}} u_{h,\tau}(x_i, s) c_{h,\tau}(x_i, s) e^{s/\epsilon} ds. \quad (3.11)$$

A direct computation gives

$$c_i^{n+1} = c_i^n e^{-\tau_{n+1} (p_i^{n+1} + p_i^n)/2}, \quad (3.12)$$

$$\begin{aligned} p_i^{n+1} &= e^{-\tau_{n+1}/\epsilon} p_i^n + \frac{1}{\tau_{n+1}} \left\{ \left(u_i^{n+1} (\epsilon - \tau_{n+1}) - u_i^n \epsilon \right) \left(c_i^{n+1} (\epsilon - \tau_{n+1}) - c_i^n \epsilon \right) \right. \\ &\quad - \left(u_i^{n+1} \epsilon - u_i^n (\epsilon + \tau_{n+1}) \right) \left(c_i^{n+1} \epsilon - c_i^n (\epsilon + \tau_{n+1}) \right) e^{-\tau_{n+1}/\epsilon} \\ &\quad \left. + (u_i^{n+1} - u_i^n) (c_i^{n+1} - c_i^n) \epsilon^2 \left(1 - e^{-\tau_{n+1}/\epsilon} \right) \right\}, \end{aligned} \quad (3.13)$$

for $i = 1, \dots, M$ and $n = 0, \dots, N-1$. Note that the effects described by the model (2.1)–(2.5), such as chemotaxis, strongly rely on the nonlinear coupling terms. Therefore, all nonlinearities are treated implicitly in the discrete problem (3.7)–(3.9).

To compute a solution of the nonlinear problem (3.7)–(3.9) at time t_{n+1} (assuming that the solution vectors \mathbf{u}^n , \mathbf{c}^n , and \mathbf{p}^n at the previous time instant t_n are known), we apply simple fixed-point iterations leading to

sequences $\mathbf{u}_k^{n+1} = (u_{j,k}^{n+1})_{j=1}^M$, $\mathbf{c}_k^{n+1} = (c_{j,k}^{n+1})_{j=1}^M$, and $\mathbf{p}_k^{n+1} = (p_{j,k}^{n+1})_{j=1}^M$. We set $\mathbf{u}_0^{n+1} = \mathbf{u}^n$, $\mathbf{c}_0^{n+1} = \mathbf{c}^n$, $\mathbf{p}_0^{n+1} = \mathbf{p}^n$ and then, for $k > 0$ and $i = 1, \dots, M$, we define

$$c_{i,k}^{n+1} = c_i^n e^{-\tau_{n+1} (p_{i,k-1}^{n+1} + p_i^n)/2}, \quad (3.14)$$

$$p_{i,k}^{n+1} = e^{-\tau_{n+1}/\epsilon} p_i^n + \frac{1}{\tau_{n+1}^2} \left\{ \begin{aligned} & \left(u_{i,k-1}^{n+1} (\epsilon - \tau_{n+1}) - u_i^n \epsilon \right) \left(c_{i,k}^{n+1} (\epsilon - \tau_{n+1}) - c_i^n \epsilon \right) \\ & - \left(u_{i,k-1}^{n+1} \epsilon - u_i^n (\epsilon + \tau_{n+1}) \right) \left(c_{i,k}^{n+1} \epsilon - c_i^n (\epsilon + \tau_{n+1}) \right) e^{-\tau_{n+1}/\epsilon} \\ & + (u_{i,k-1}^{n+1} - u_i^n) (c_{i,k}^{n+1} - c_i^n) \epsilon^2 \left(1 - e^{-\tau_{n+1}/\epsilon} \right) \end{aligned} \right\}. \quad (3.15)$$

The iterate \mathbf{u}_k^{n+1} is computed by solving the linear system

$$(\mathbb{M} + \theta \tau_{n+1} \mathbb{A}_{k-1}^{n+1}) \mathbf{u}_k^{n+1} = (\mathbb{M} - (1 - \theta) \tau_{n+1} \mathbb{A}^n) \mathbf{u}^n, \quad (3.16)$$

where the matrix \mathbb{A}_{k-1}^{n+1} is defined by

$$\mathbb{A}_{k-1}^{n+1} = \left(-\mu (\phi_j (1 - u_{h,k-1}^{n+1}), \phi_i) - \chi (\phi_j \nabla c_{h,k}^{n+1}, \nabla \phi_i) \right)_{i,j=1}^M \quad (3.17)$$

and $u_{h,k-1}^{n+1} = \pi_h \mathbf{u}_{k-1}^{n+1}$ and $c_{h,k}^{n+1} = \pi_h \mathbf{c}_k^{n+1}$ are the finite element functions corresponding to the coefficient vectors \mathbf{u}_{k-1}^{n+1} and \mathbf{c}_k^{n+1} , respectively.

The linear system (3.16) has the form

$$\mathbb{B} \mathbf{u}^{n+1} = \mathbb{K} \mathbf{u}^n \quad (3.18)$$

and it is desirable that this system is positivity preserving, i.e., that $\mathbf{u}^{n+1} \geq 0$ if $\mathbf{u}^n \geq 0$. A necessary and sufficient condition for this property is $\mathbb{B}^{-1} \mathbb{K} \geq 0$ but this condition is difficult to verify. Sufficient conditions are formulated in the following lemma. Note that, throughout the paper, an inequality of the type $\mathbf{u}^n \geq 0$ means that the inequality holds for each component of the vector \mathbf{u}^n . Similarly, the fact that all entries of a matrix \mathbb{K} are non-negative is expressed by $\mathbb{K} \geq 0$.

Lemma 3.1. *Let the matrices $\mathbb{B} = (b_{ij})_{i,j=1}^M$ and $\mathbb{K} = (k_{ij})_{i,j=1}^M$ satisfy*

$$b_{ii} \geq 0, \quad k_{ii} \geq 0, \quad b_{ij} \leq 0, \quad k_{ij} \geq 0, \quad \forall i, j = 1, \dots, M, \quad i \neq j,$$

and let \mathbb{B} be a strictly diagonally dominant or an irreducibly diagonally dominant matrix. Then \mathbb{B} is an M-matrix and the scheme (3.18) is positivity preserving.

PROOF. According to [53, Theorem 3.27], \mathbb{B} is an M-matrix. Thus, $\mathbb{B}^{-1} \geq 0$ and hence also $\mathbb{B}^{-1} \mathbb{K} \geq 0$, which implies the result. \square

In general, the linear system (3.16) originating from a standard Galerkin discretization does not satisfy the above constraints because the mass matrix is non-negative and the stiffness matrix may contain positive off-diagonal entries. Our numerical results in Section 6 show that indeed the concentration \mathbf{u} may become negative in some parts of the computational domain Ω .

4 FCT stabilization

As we will see in Section 6, the magnitude of the solutions gradients can be extremely large in some regions. The solution of the Galerkin discretization from the previous section may become negative especially in these regions. As a remedy, in the following we will modify the Galerkin discretization to guarantee a positivity preservation property. As shown by Kuzmin [33, 34, 32], this property can be readily enforced at the discrete level using a conservative manipulation of the mass and stiffness matrices. The former will be approximated by its diagonal counterpart \mathbb{M}_L constructed using row-sum mass lumping, whereas the latter will be modified by adding an artificial diffusion matrix. To limit the amount of the artificial diffusion, the FEM-FCT approach will be applied following [34].

Since the methods considered in this section guarantee that the approximate solutions are non-negative, it is possible to replace the matrix \mathbb{A}^n from the previous section by $\tilde{\mathbb{A}}^n = (\tilde{a}_{ij}^n)_{i,j=1}^M$ with

$$\tilde{a}_{ij}^n = -\mu (\phi_j(1 - |u_h^n|), \phi_i) - \chi (\phi_j \nabla c_h^n, \nabla \phi_i).$$

The matrix $\tilde{\mathbb{A}}^n$ is more suitable for theoretical considerations than the matrix \mathbb{A}^n . However, a non-negative approximate solution u_h^n, c_h^n, p_h^n satisfying a discrete problem based on the matrix $\tilde{\mathbb{A}}^n$ will satisfy also the corresponding discrete problem with the original matrix \mathbb{A}^n .

Using the matrix $\tilde{\mathbb{A}}^n$, we introduce a symmetric artificial diffusion matrix $\mathbb{D}^n = (d_{ij}^n)_{i,j=1}^M$ defined by

$$d_{ij}^n = -\max\{\tilde{a}_{ij}^n, 0, \tilde{a}_{ji}^n\} \quad \text{for } i \neq j, \quad d_{ii}^n = -\sum_{j=1, j \neq i}^M d_{ij}^n,$$

and we set $\mathbb{L}^n = \tilde{\mathbb{A}}^n + \mathbb{D}^n$. Note that $\mathbb{L}^n = (l_{ij}^n)_{i,j=1}^M$ is a Z-matrix (i.e., it has non-positive off-diagonal entries). Furthermore, we introduce the lumped mass matrix $\mathbb{M}_L = \text{diag}(m_1, \dots, m_M)$ with

$$m_i = \sum_{j=1}^M m_{ij}, \quad i = 1, \dots, M.$$

Now, the simplest way to enforce the positivity preservation is to consider the so-called low-order method corresponding to the so-called high-order method (3.7) which is defined by

$$(\mathbb{M}_L + \theta \tau_{n+1} \mathbb{L}^{n+1}) \mathbf{u}^{n+1} = (\mathbb{M}_L - (1 - \theta) \tau_{n+1} \mathbb{L}^n) \mathbf{u}^n, \quad n = 0, \dots, N-1. \quad (4.1)$$

Note that the matrix \mathbb{L}^{n+1} depends on \mathbf{u}^{n+1} and \mathbf{c}^{n+1} so that the low-order problem is again nonlinear. In contrast to the Galerkin discretization (3.7), it is now possible to assure the positivity preservation for sufficiently small time steps.

Lemma 4.1. *Let the time step τ_{n+1} satisfy the conditions*

$$(1 - \theta) \tau_{n+1} l_{ii}^n \leq m_i, \quad \theta \tau_{n+1} \left(\mu m_i + \chi (\nabla c_h^{n+1}, \nabla \phi_i) \right) < m_i, \quad i = 1, \dots, M. \quad (4.2)$$

Then the matrix $\mathbb{M}_L - (1 - \theta) \tau_{n+1} \mathbb{L}^n$ has non-negative entries and $\mathbb{M}_L + \theta \tau_{n+1} \mathbb{L}^{n+1}$ is an M-matrix.

PROOF. The first condition in (4.2) implies that $\mathbb{M}_L - (1 - \theta) \tau_{n+1} \mathbb{L}^n$ has non-negative diagonal entries. The off-diagonal entries of this matrix are non-negative as well, since \mathbb{M}_L is diagonal and \mathbb{L}^n is a Z-matrix.

Denoting $\mathbb{B} = \mathbb{M}_L + \theta \tau_{n+1} \mathbb{L}^{n+1}$, one has for any $i \in \{1, \dots, M\}$

$$\sum_{j=1}^M b_{ij} = m_i + \theta \tau_{n+1} \sum_{j=1}^M \tilde{a}_{ij}^{n+1} = m_i - \theta \tau_{n+1} \left(\mu (1 - |u_h^{n+1}|, \phi_i) + \chi (\nabla c_h^{n+1}, \nabla \phi_i) \right),$$

where we used the fact that $\sum_{j=1}^M \phi_j = 1$. Since $(1, \phi_i) = m_i$, it follows from the second condition in (4.2) that $\sum_{j=1}^M b_{ij} > 0$. Thus, $b_{ii} > \sum_{j \neq i} |b_{ij}|$, i.e., \mathbb{B} is strictly diagonally dominant and hence non-singular. Moreover, \mathbb{B} is a matrix of non-negative type and hence it is an M-matrix (see, e.g., [6, Corollary 3.13]). \square

Corollary 4.2. *Let the time step τ_{n+1} satisfy the conditions (4.2). Then the low-order scheme (4.1) is positivity preserving, i.e.,*

$$\mathbf{u}^n \geq 0 \quad \Rightarrow \quad \mathbf{u}^{n+1} \geq 0. \quad (4.3)$$

PROOF. According to Lemma 4.1, the matrix $\mathbb{M}_L + \theta \tau_{n+1} \mathbb{L}^{n+1}$ is non-singular, $(\mathbb{M}_L + \theta \tau_{n+1} \mathbb{L}^{n+1})^{-1} \geq 0$, and $\mathbb{M}_L - (1 - \theta) \tau_{n+1} \mathbb{L}^n \geq 0$, which immediately implies (4.3). \square

Remark 4.3. The second condition in (4.2) involves c_h^{n+1} which implicitly depends on τ_{n+1} through \mathbf{p}^{n+1} and hence also through \mathbf{u}^{n+1} . Therefore, it is desirable to replace this condition by a condition independent of c_h^{n+1} . This is possible since we will show that the values of c_h^{n+1} are in the interval $[0, 1]$. Then, employing (3.4), one gets

$$(\nabla c_h^{n+1}, \nabla \phi_i) = \sum_{j=1}^M c_j^{n+1} (\nabla \phi_j, \nabla \phi_i) \leq \sum_{K \ni x_i} \sum_{j=1}^M \|\nabla \phi_j\|_{L^2(K)} \|\nabla \phi_i\|_{L^2(K)} \leq n_v \kappa^2 \sum_{K \ni x_i} h_K^{d-2},$$

where n_v is the number of vertices of a cell in \mathcal{T}_h ($n_v = d + 1$ for simplices, $n_v = 4$ for quadrilaterals, and $n_v = 8$ for hexahedra). Thus, if the time step τ_{n+1} satisfies

$$\theta \tau_{n+1} \left(\mu m_i + \chi n_v \kappa^2 \sum_{K \ni x_i} h_K^{d-2} \right) < m_i, \quad i = 1, \dots, M, \quad (4.4)$$

and $c_h^{n+1} \in [0, 1]$, then the second condition in (4.2) holds. Note that (4.4) may be significantly more restrictive than (4.2).

To prove that the low-order discretization consisting of the equations (4.1), (3.12), and (3.13) has a solution, we shall use the following consequence of Brouwer's fixed-point theorem.

Lemma 4.4. *Let X be a finite-dimensional Hilbert space with inner product $(\cdot, \cdot)_X$ and norm $\|\cdot\|_X$. Let $P : X \rightarrow X$ be a continuous mapping and $K > 0$ a real number such that $(Px, x)_X > 0$ for any $x \in X$ with $\|x\|_X = K$. Then there exists $x \in X$ such that $\|x\|_X < K$ and $Px = 0$.*

PROOF. See [50, p. 164, Lemma 1.4]. \square

Theorem 4.5. *Consider any $n \in \{0, \dots, N - 1\}$ and let $\mathbf{u}^n, \mathbf{c}^n, \mathbf{p}^n \in \mathbb{R}^M$ satisfy $\mathbf{u}^n \geq 0$, $1 \geq \mathbf{c}^n \geq 0$, $\mathbf{p}^n \geq 0$. Let the time step τ_{n+1} satisfy the conditions*

$$(1 - \theta) \tau_{n+1} l_{ii}^n \leq m_i, \quad \theta \tau_{n+1} \left(\mu m_i + \chi n_v \kappa^2 \sum_{K \ni x_i} h_K^{d-2} \right) < m_i, \quad i = 1, \dots, M. \quad (4.5)$$

Then there exist vectors $\mathbf{u}^{n+1}, \mathbf{c}^{n+1}, \mathbf{p}^{n+1} \in \mathbb{R}^M$ satisfying (4.1), (3.12), (3.13) and $\mathbf{u}^{n+1} \geq 0$, $1 \geq \mathbf{c}^{n+1} \geq 0$, $\mathbf{p}^{n+1} \geq 0$.

PROOF. To get rid of the exponential dependence on \mathbf{p}^{n+1} when estimating the nonlinear terms in (4.1), we replace (3.12) by

$$c_i^{n+1} = c_i^n e^{-\tau_{n+1} (|p_i^{n+1}| + p_i^n)/2}, \quad i = 1, \dots, M. \quad (4.6)$$

At the end of the proof, we will show that $\mathbf{p}^{n+1} \geq 0$ so that the original relation (3.12) will be recovered.

For $u, p \in \mathbb{R}$ and $i = 1, \dots, M$, we introduce the notation

$$C_i(p) = c_i^n e^{-\tau_{n+1} (|p| + p_i^n)/2} \quad (4.7)$$

and

$$\begin{aligned} P_i(u, p) &= \frac{1}{\tau_{n+1}^2} u C_i(p) \left\{ (\epsilon - \tau_{n+1})^2 + \epsilon^2 (1 - 2e^{-\tau_{n+1}/\epsilon}) \right\} \\ &\quad + \frac{\epsilon}{\tau_{n+1}^2} u c_i^n \left\{ \tau_{n+1} (1 + e^{-\tau_{n+1}/\epsilon}) - 2\epsilon (1 - e^{-\tau_{n+1}/\epsilon}) \right\} \\ &\quad + \frac{\epsilon}{\tau_{n+1}^2} u_i^n C_i(p) \left\{ \tau_{n+1} (1 + e^{-\tau_{n+1}/\epsilon}) - 2\epsilon (1 - e^{-\tau_{n+1}/\epsilon}) \right\} \\ &\quad + \frac{1}{\tau_{n+1}^2} u_i^n c_i^n \left\{ \epsilon^2 (2 - e^{-\tau_{n+1}/\epsilon}) - (\epsilon + \tau_{n+1})^2 e^{-\tau_{n+1}/\epsilon} \right\} + e^{-\tau_{n+1}/\epsilon} p_i^n. \end{aligned} \quad (4.8)$$

Then, the validity of (4.6) and (3.13) is equivalent to

$$c_i^{n+1} = C_i(p_i^{n+1}), \quad p_i^{n+1} = P_i(u_i^{n+1}, p_i^{n+1}), \quad i = 1, \dots, M.$$

Note that

$$|P_i(u, p)| \leq (|u| + u_i^n) c_i^n \left(\frac{2\epsilon + \tau_{n+1}}{\tau_{n+1}} \right)^2 + p_i^n \quad \forall u, p \in \mathbb{R}, \quad i = 1, \dots, M. \quad (4.9)$$

Furthermore, for $\mathbf{u}, \mathbf{p} \in \mathbb{R}^M$ and $i, j = 1, \dots, M$, we denote

$$A_{ij}(\mathbf{u}, \mathbf{p}) = -\mu (\phi_j(1 - |\pi_h \mathbf{u}|), \phi_i) - \chi (\phi_j \nabla(\pi_h \mathbf{C}(\mathbf{p})), \nabla \phi_i), \quad (4.10)$$

$$D_{ij}(\mathbf{u}, \mathbf{p}) = -\max\{A_{ij}(\mathbf{u}, \mathbf{p}), 0, A_{ji}(\mathbf{u}, \mathbf{p})\} \quad \text{for } i \neq j, \quad D_{ii}(\mathbf{u}, \mathbf{p}) = -\sum_{j=1, j \neq i}^M D_{ij}(\mathbf{u}, \mathbf{p}), \quad (4.11)$$

$$S_i(\mathbf{u}, \mathbf{p}) = m_i u_i + \theta \tau_{n+1} \sum_{j=1}^M (A_{ij}(\mathbf{u}, \mathbf{p}) + D_{ij}(\mathbf{u}, \mathbf{p})) u_j - [(\mathbb{M}_L - (1 - \theta) \tau_{n+1} \mathbb{L}^n) \mathbf{u}^n]_i, \quad (4.12)$$

where $\mathbf{C}(\mathbf{p}) = (C_i(p_i))_{i=1}^M$. Then (4.1) with c_h^{n+1} defined by (4.6) is equivalent to

$$S_i(\mathbf{u}^{n+1}, \mathbf{p}^{n+1}) = 0, \quad i = 1, \dots, M.$$

Therefore, defining the operator $P : \mathbb{R}^{2M} \rightarrow \mathbb{R}^{2M}$ by

$$P\mathbf{U} = (S_1(\mathbf{u}, \mathbf{p}), \dots, S_M(\mathbf{u}, \mathbf{p}), p_1 - P_1(u_1, p_1), \dots, p_M - P_M(u_M, p_M)) \quad \forall \mathbf{U} = (\mathbf{u}, \mathbf{p}) \in \mathbb{R}^{2M}, \quad (4.13)$$

the vectors \mathbf{u}^{n+1} , \mathbf{c}^{n+1} , \mathbf{p}^{n+1} are a solution of (4.1), (4.6), (3.13) if and only if $\mathbf{U} = (\mathbf{u}^{n+1}, \mathbf{p}^{n+1})$ satisfies $P\mathbf{U} = 0$ and $\mathbf{c}^{n+1} = \mathbf{C}(\mathbf{p}^{n+1})$.

To show that the equation $P\mathbf{U} = 0$ has a solution, we will verify the assumptions of Lemma 4.4. Since it is obvious that the operator P is continuous, it suffices to investigate the product $(P\mathbf{U}, \mathbf{U})$, where (\cdot, \cdot) is

the Euclidean inner product in \mathbb{R}^{2M} . We will denote the corresponding norm by $\|\cdot\|$. The Euclidean norm in \mathbb{R}^M will be denoted by $\|\cdot\|_M$. Since the matrix $(D_{ij}(\mathbf{u}, \mathbf{p}))_{i,j=1}^M$ is symmetric and has zero row sums and non-positive off-diagonal entries, one obtains

$$\sum_{i,j=1}^M u_i D_{ij}(\mathbf{u}, \mathbf{p}) u_j = -\frac{1}{2} \sum_{i,j=1}^M D_{ij}(\mathbf{u}, \mathbf{p}) (u_i - u_j)^2 \geq 0 \quad \forall \mathbf{u}, \mathbf{p} \in \mathbb{R}^M.$$

Furthermore, since $0 \leq \mathbf{C}(\mathbf{p}) \leq 1$, the expressions $(\phi_j \nabla(\pi_h \mathbf{C}(\mathbf{p})), \nabla \phi_i)$ can be bounded independently of \mathbf{p} . Therefore, using the equivalence of norms on finite-dimensional spaces, one obtains

$$\theta \tau_{n+1} \sum_{i,j=1}^M u_i (A_{ij}(\mathbf{u}, \mathbf{p}) + D_{ij}(\mathbf{u}, \mathbf{p})) u_j \geq \theta \tau_{n+1} \mu \|\pi_h \mathbf{u}\|_{L^3(\Omega)}^3 - C_1 \|\mathbf{u}\|_M^2 \geq C_2 \|\mathbf{u}\|_M^3 - C_1 \|\mathbf{u}\|_M^2,$$

where C_1 and C_2 are positive constants independent of \mathbf{u} and \mathbf{p} . Thus,

$$\sum_{i=1}^M u_i S_i(\mathbf{u}, \mathbf{p}) \geq C_2 \|\mathbf{u}\|_M^3 - C_1 \|\mathbf{u}\|_M^2 - C_3 \|\mathbf{u}\|_M, \quad (4.14)$$

where $C_3 = \|(\mathbb{M}_L - (1 - \theta) \tau_{n+1} \mathbb{L}^n) \mathbf{u}^n\|_M$. Finally, using (4.9), it follows that

$$\sum_{i=1}^M p_i (p_i - P_i(u_i, p_i)) \geq \|\mathbf{p}\|_M^2 - C_4 \|\mathbf{p}\|_M \|\mathbf{u}\|_M - C_5 \|\mathbf{p}\|_M$$

with positive constants C_4 and C_5 independent of \mathbf{u} and \mathbf{p} . Applying the Young inequality, the previous two inequalities imply that there exist positive constants C_6 and C_7 such that

$$(P \mathbf{U}, \mathbf{U}) \geq \frac{1}{2} \|\mathbf{U}\|^2 + C_2 \|\mathbf{u}\|_M^3 - C_6 \|\mathbf{u}\|_M^2 - C_7 \geq \frac{1}{2} \|\mathbf{U}\|^2 - \frac{C_6^3}{C_2^2} - C_7 \quad \forall \mathbf{U} = (\mathbf{u}, \mathbf{p}) \in \mathbb{R}^{2M}.$$

Thus, for any $K > \sqrt{2C_6^3/C_2^2 + 2C_7}$, one has $(P \mathbf{U}, \mathbf{U}) > 0$ for any $\mathbf{U} \in \mathbb{R}^{2M}$ with $\|\mathbf{U}\| = K$. Therefore, according to Lemma 4.4, there exists a solution \mathbf{U} of the equation $P \mathbf{U} = 0$ and hence also a solution \mathbf{u}^{n+1} , \mathbf{c}^{n+1} , \mathbf{p}^{n+1} of (4.1), (4.6), and (3.13).

It immediately follows from (4.6) that $0 \leq \mathbf{c}^{n+1} \leq 1$. Thus, according to Corollary 4.2 and Remark 4.3, the solution satisfies $\mathbf{u}^{n+1} \geq 0$. Since (3.13) is equivalent to (3.11), one also has $\mathbf{p}^{n+1} \geq 0$ and hence (3.12) is satisfied as well. \square

Although the solution of (4.1), (3.12), (3.13) does not possess negative values under the time step restrictions (4.2), it is usually very inaccurate since too much artificial diffusion is introduced by the modifications leading to the low-order method (4.1), cf. Section 6.3. Therefore, in the FEM-FCT methodology, a correction term $\tilde{\mathbf{f}}^{n+1}$ is added in such a way that the method becomes less diffusive while negative values are still excluded. This leads to an extension of (4.1) in the form

$$(\mathbb{M}_L + \theta \tau_{n+1} \mathbb{L}^{n+1}) \mathbf{u}^{n+1} = (\mathbb{M}_L - (1 - \theta) \tau_{n+1} \mathbb{L}^n) \mathbf{u}^n + \tilde{\mathbf{f}}^{n+1}.$$

The high-order method (3.7) (with \mathbb{A}^n replaced by $\tilde{\mathbb{A}}^n$) is recovered if

$$\tilde{\mathbf{f}}^{n+1} = (\mathbb{M}_L - \mathbb{M})(\mathbf{u}^{n+1} - \mathbf{u}^n) + \theta \tau_{n+1} \mathbb{D}^{n+1} \mathbf{u}^{n+1} + (1 - \theta) \tau_{n+1} \mathbb{D}^n \mathbf{u}^n. \quad (4.15)$$

Since \mathbb{D}^n has zero row sums, one can write

$$(\mathbb{D}^n \mathbf{u}^n)_i = \sum_{j=1}^M d_{ij}^n (u_j^n - u_i^n), \quad i = 1, \dots, M.$$

For the terms with the matrices \mathbb{D}^{n+1} and $\mathbb{M}_L - \mathbb{M}$ (which also have zero row sums), one can proceed analogously and hence (4.15) holds if an only if

$$\bar{\mathbf{f}}^{n+1} = \left(\sum_{j=1}^M f_{ij}^{n+1} \right)_{i=1}^M,$$

where the algebraic fluxes f_{ij}^{n+1} are given by

$$f_{ij}^{n+1} = -m_{ij} (u_j^{n+1} - u_i^{n+1}) + m_{ij} (u_j^n - u_i^n) + \theta \tau_{n+1} d_{ij}^{n+1} (u_j^{n+1} - u_i^{n+1}) + (1 - \theta) \tau_{n+1} d_{ij}^n (u_j^n - u_i^n). \quad (4.16)$$

Because \mathbb{M} , \mathbb{D}^{n+1} , and \mathbb{D}^n are symmetric matrices, one has $f_{ij}^{n+1} = -f_{ji}^{n+1}$. Note also that the fluxes depend on (unknown) values of the approximate solution at time level t_{n+1} .

Now, the idea of the FCT approach is to limit the fluxes f_{ij}^{n+1} by solution dependent correction factors $\alpha_{ij}^{n+1} \in [0, 1]$ called limiters so that the non-negativity of the approximate solution can be guaranteed but less artificial diffusion is introduced than in case of the low-order method. This leads to the discrete problem

$$(\mathbb{M}_L + \theta \tau_{n+1} \mathbb{L}^{n+1}) \mathbf{u}^{n+1} = (\mathbb{M}_L - (1 - \theta) \tau_{n+1} \mathbb{L}^n) \mathbf{u}^n + \left(\sum_{j=1}^M \alpha_{ij}^{n+1} f_{ij}^{n+1} \right)_{i=1}^M. \quad (4.17)$$

The original Galerkin discretization is recovered for $\alpha_{ij} = 1$ while the largest amount of artificial diffusion is introduced for $\alpha_{ij} = 0$. The latter setting is appropriate in the neighborhood of steep fronts and large gradients. The artificial diffusion can be removed in regions where the solution is smooth and where non-positive off-diagonal entries of the stiffness matrix do not pose any threat to non-negativity. The corrected fluxes depend on the approximate solution in a nonlinear way but since the problem in here is already nonlinear, we can treat both nonlinearities simultaneously.

It is convenient to write the nonlinear problem (4.17) in the form

$$\mathbb{M}_L \bar{\mathbf{u}} = (\mathbb{M}_L - (1 - \theta) \tau_{n+1} \mathbb{L}^n) \mathbf{u}^n, \quad (4.18)$$

$$\mathbb{M}_L \tilde{\mathbf{u}} = \mathbb{M}_L \bar{\mathbf{u}} + \left(\sum_{j=1}^M \alpha_{ij}^{n+1} f_{ij}^{n+1} \right)_{i=1}^M, \quad (4.19)$$

$$(\mathbb{M}_L + \theta \tau_{n+1} \mathbb{L}^{n+1}) \mathbf{u}^{n+1} = \mathbb{M}_L \tilde{\mathbf{u}}. \quad (4.20)$$

According to Lemma 4.1, the steps (4.18) and (4.20) are positivity preserving under the conditions (4.2). To guarantee the positivity preservation of the second step, the limiters α_{ij}^{n+1} have to be defined appropriately. We will apply the Zalesak algorithm [55] which will be described next.

The solution of the nonlinear problem (4.18)–(4.20) is computed by fixed-point iterations where the algebraic fluxes are calculated using the previous iterate. Since the properties of the Zalesak algorithm do not depend on the form of these fluxes, we will denote them simply by f_{ij} . Then, the aim is to find limiters $\alpha_{ij} \in [0, 1]$ such that the solution $\tilde{\mathbf{u}}$ of

$$\mathbb{M}_L \tilde{\mathbf{u}} = \mathbb{M}_L \bar{\mathbf{u}} + \left(\sum_{j=1}^M \alpha_{ij} f_{ij} \right)_{i=1}^M$$

satisfies

$$\bar{u}_i^{\min} \leq \tilde{u}_i \leq \bar{u}_i^{\max}, \quad i = 1, \dots, M, \quad (4.21)$$

where

$$\bar{u}_i^{\min} = \min_{j \in \mathcal{N}_i \cup \{i\}} \bar{u}_j, \quad \bar{u}_i^{\max} = \max_{j \in \mathcal{N}_i \cup \{i\}} \bar{u}_j, \quad i = 1, \dots, M,$$

and \mathcal{N}_i is the index set of neighbour vertices to the vertex x_i (note that two vertices of the triangulation \mathcal{T}_h are called neighbouring if they are contained in the same mesh cell). To preserve conservativity, it is important that the limiters α_{ij} form a symmetric matrix. The limiting process begins with cancelling all fluxes that are diffusive in nature and tend to flatten the solution profiles, cf. [34]. The required modification is

$$f_{ij} := 0 \quad \text{if } f_{ij}(\bar{u}_j - \bar{u}_i) > 0. \quad (4.22)$$

The remaining fluxes are truly antidiffusive and the computation of α_{ij} involves the following steps:

1. Compute the sum of positive/negative antidiffusive fluxes into node i

$$P_i^+ = \sum_{j \in \mathcal{N}_i} \max\{0, f_{ij}\}, \quad P_i^- = \sum_{j \in \mathcal{N}_i} \min\{0, f_{ij}\}. \quad (4.23)$$

2. Compute the distance to a local extremum of the auxiliary solution $\bar{\mathbf{u}}$

$$Q_i^+ = m_i(\bar{u}_i^{\max} - \bar{u}_i), \quad Q_i^- = m_i(\bar{u}_i^{\min} - \bar{u}_i). \quad (4.24)$$

3. Compute the nodal correction factors for the net increment to node i

$$R_i^+ = \min\left\{1, \frac{Q_i^+}{P_i^+}\right\}, \quad R_i^- = \min\left\{1, \frac{Q_i^-}{P_i^-}\right\}. \quad (4.25)$$

If a denominator is zero, set the respective value of R_i^+ or R_i^- equal to 1.

4. Check the sign of the antidiffusive flux and define the correction factor by

$$\alpha_{ij} = \begin{cases} \min\{R_i^+, R_j^-\} & \text{if } f_{ij} > 0, \\ 1 & \text{if } f_{ij} = 0, \\ \min\{R_i^-, R_j^+\} & \text{if } f_{ij} < 0. \end{cases} \quad (4.26)$$

It can be easily verified (see, e.g., [6]) that this algorithm leads to the property (4.21).

Now we are in a position to prove the solvability and positivity preservation for the above FCT discretization.

Theorem 4.6. *Consider any $n \in \{0, \dots, N-1\}$ and let $\mathbf{u}^n, \mathbf{c}^n, \mathbf{p}^n \in \mathbb{R}^M$ satisfy $\mathbf{u}^n \geq 0$, $1 \geq \mathbf{c}^n \geq 0$, $\mathbf{p}^n \geq 0$. Let the time step τ_{n+1} satisfy the conditions (4.5). Then there exist vectors $\mathbf{u}^{n+1}, \mathbf{c}^{n+1}, \mathbf{p}^{n+1} \in \mathbb{R}^M$ satisfying (4.17), (3.12), (3.13) where the fluxes f_{ij}^{n+1} are given by (4.16) and (4.22) and the limiters α_{ij}^{n+1} are computed using the Zalesak algorithm (4.23)–(4.26) from the fluxes f_{ij}^{n+1} . Moreover, these vectors satisfy $\mathbf{u}^{n+1} \geq 0$, $1 \geq \mathbf{c}^{n+1} \geq 0$, and $\mathbf{p}^{n+1} \geq 0$.*

PROOF. The proof follows the lines of that of Theorem 4.5. Thus, we again start with replacing (3.12) by (4.6). We again define C_i, P_i, A_{ij} , and D_{ij} by (4.7), (4.8), (4.10) and (4.11), respectively, whereas S_i are now defined by

$$S_i(\mathbf{u}, \mathbf{p}) = m_i u_i + \theta \tau_{n+1} \sum_{j=1}^M (A_{ij}(\mathbf{u}, \mathbf{p}) + D_{ij}(\mathbf{u}, \mathbf{p})) u_j - \sum_{j=1}^M \alpha_{ij}(\mathbf{u}, \mathbf{p}) \tilde{f}_{ij}(\mathbf{u}, \mathbf{p}) - [(\mathbb{M}_L - (1 - \theta) \tau_{n+1} \mathbb{L}^n) \mathbf{u}^n]_i,$$

where $\alpha_{ij}(\mathbf{u}, \mathbf{p})$ are defined by the Zalesak algorithm (4.23)–(4.26) for the algebraic fluxes $\tilde{f}_{ij}(\mathbf{u}, \mathbf{p})$ defined by

$$\tilde{f}_{ij}(\mathbf{u}, \mathbf{p}) = \begin{cases} f_{ij}(\mathbf{u}, \mathbf{p}) & \text{if } f_{ij}(\mathbf{u}, \mathbf{p})(\bar{u}_j - \bar{u}_i) \leq 0, \\ 0 & \text{if } f_{ij}(\mathbf{u}, \mathbf{p})(\bar{u}_j - \bar{u}_i) > 0, \end{cases}$$

with $\bar{\mathbf{u}}$ from (4.18) and

$$f_{ij}(\mathbf{u}, \mathbf{p}) = (-m_{ij} + \theta \tau_{n+1} D_{ij}(\mathbf{u}, \mathbf{p}))(u_j - u_i) + (m_{ij} + (1 - \theta) \tau_{n+1} d_{ij}^n)(u_j^n - u_i^n).$$

Then, defining the operator $P : \mathbb{R}^{2M} \rightarrow \mathbb{R}^{2M}$ by (4.13), the vectors \mathbf{u}^{n+1} , \mathbf{c}^{n+1} , \mathbf{p}^{n+1} are a solution of (4.17), (4.6), (3.13) if and only if $\mathbf{U} = (\mathbf{u}^{n+1}, \mathbf{p}^{n+1})$ satisfies $P\mathbf{U} = 0$ and $\mathbf{c}^{n+1} = \mathbf{C}(\mathbf{p}^{n+1})$.

The solvability of the equation $P\mathbf{U} = 0$ will be again proved using Lemma 4.4. To show the continuity of the operator P at any point $\tilde{\mathbf{U}} \equiv (\tilde{\mathbf{u}}, \tilde{\mathbf{p}}) \in \mathbb{R}^{2M}$, it suffices to consider the terms $\alpha_{ij}(\mathbf{u}, \mathbf{p}) \tilde{f}_{ij}(\mathbf{u}, \mathbf{p})$ since the remaining terms in the definition of P are clearly continuous. Moreover, f_{ij} and hence also \tilde{f}_{ij} are continuous. Thus, if $\tilde{f}_{ij}(\tilde{\mathbf{U}}) \neq 0$, then the denominators in the formulas defining $\alpha_{ij}(\mathbf{U})$ with $\mathbf{U} = (\mathbf{u}, \mathbf{p})$ do not vanish in a neighborhood of $\tilde{\mathbf{U}}$ and hence α_{ij} is continuous at $\tilde{\mathbf{U}}$. Consequently, also $\alpha_{ij} \tilde{f}_{ij}$ is continuous at $\tilde{\mathbf{U}}$. If $\tilde{f}_{ij}(\tilde{\mathbf{U}}) = 0$, then

$$|(\alpha_{ij} \tilde{f}_{ij})(\mathbf{U}) - (\alpha_{ij} \tilde{f}_{ij})(\tilde{\mathbf{U}})| = |(\alpha_{ij} \tilde{f}_{ij})(\mathbf{U})| \leq |\tilde{f}_{ij}(\mathbf{U})| = |\tilde{f}_{ij}(\mathbf{U}) - \tilde{f}_{ij}(\tilde{\mathbf{U}})|,$$

which shows that $\alpha_{ij} \tilde{f}_{ij}$ is again continuous at $\tilde{\mathbf{U}}$.

To estimate $(P\mathbf{U}, \mathbf{U})$ from below, let us denote

$$\tilde{\alpha}_{ij}(\mathbf{u}, \mathbf{p}) = \begin{cases} \alpha_{ij}(\mathbf{u}, \mathbf{p}) & \text{if } f_{ij}(\mathbf{u}, \mathbf{p})(\bar{u}_j - \bar{u}_i) \leq 0, \\ 0 & \text{if } f_{ij}(\mathbf{u}, \mathbf{p})(\bar{u}_j - \bar{u}_i) > 0. \end{cases}$$

Then $\tilde{\alpha}_{ij}$ again form a symmetric matrix and $\alpha_{ij} \tilde{f}_{ij} = \tilde{\alpha}_{ij} f_{ij}$. Therefore, $S_i(\mathbf{u}, \mathbf{p})$ can be written in the form

$$\begin{aligned} S_i(\mathbf{u}, \mathbf{p}) &= \sum_{j=1}^M m_{ij} u_j + \theta \tau_{n+1} \sum_{j=1}^M A_{ij}(\mathbf{u}, \mathbf{p}) u_j \\ &\quad + \sum_{j=1}^M (1 - \tilde{\alpha}_{ij}(\mathbf{u}, \mathbf{p})) (-m_{ij} + \theta \tau_{n+1} D_{ij}(\mathbf{u}, \mathbf{p}))(u_j - u_i) \\ &\quad + \sum_{j=1}^M (1 - \tilde{\alpha}_{ij}(\mathbf{u}, \mathbf{p})) (m_{ij} + (1 - \theta) \tau_{n+1} d_{ij}^n)(u_j^n - u_i^n) \\ &\quad - [(\mathbb{M} - (1 - \theta) \tau_{n+1} \mathbb{A}^n) \mathbf{u}^n]_i. \end{aligned}$$

Denoting $B_{ij} = (1 - \tilde{\alpha}_{ij}(\mathbf{u}, \mathbf{p})) (-m_{ij} + \theta \tau_{n+1} D_{ij}(\mathbf{u}, \mathbf{p}))$, one has

$$\sum_{i,j=1}^M u_i (1 - \tilde{\alpha}_{ij}(\mathbf{u}, \mathbf{p})) (-m_{ij} + \theta \tau_{n+1} D_{ij}(\mathbf{u}, \mathbf{p}))(u_j - u_i) = -\frac{1}{2} \sum_{i,j=1}^M B_{ij} (u_i - u_j)^2 \geq 0,$$

since the matrix $(B_{ij})_{i,j=1}^M$ is symmetric and has non-positive off-diagonal entries. Therefore, one again obtains (4.14) where the constants C_1 , C_2 are the same as in the proof of Theorem 4.5 and

$$C_3 = \|\mathbf{g}\|_M + \|(\mathbb{M} - (1 - \theta) \tau_{n+1} \mathbb{A}^n) \mathbf{u}^n\|_M,$$

where

$$g_i = \sum_{j=1}^M |m_{ij} + (1 - \theta) \tau_{n+1} d_{ij}^n| |u_j^n - u_i^n|, \quad i = 1, \dots, M.$$

Thus, in the same way as in the proof of Theorem 4.5, one concludes that there exists a solution \mathbf{U} of the equation $P\mathbf{U} = 0$ and hence also a solution \mathbf{u}^{n+1} , \mathbf{c}^{n+1} , \mathbf{p}^{n+1} of (4.17), (4.6), and (3.13).

To prove the positivity preservation, we write (4.17) in the form (4.18)–(4.20). Since $\mathbb{M}_L - (1 - \theta) \tau_{n+1} \mathbb{L}^n \geq 0$ according to Lemma 4.1, one has $\bar{\mathbf{u}} \geq 0$. Applying (4.21), one gets $\tilde{\mathbf{u}} \geq 0$. Since $0 \leq \mathbf{c}^{n+1} \leq 1$ due to (4.6), it follows from Lemma 4.1 and Remark 4.3 that the matrix $\mathbb{M}_L + \theta \tau_{n+1} \mathbb{L}^{n+1}$ is an M-matrix. Consequently, $\mathbf{u}^{n+1} \geq 0$ in view of (4.20). Since (3.13) is equivalent to (3.11), one also has $\mathbf{p}^{n+1} \geq 0$ and hence (3.12) is satisfied as well. \square

5 Iterative solution of the FCT discretization

To compute a solution of the nonlinear problem (4.17), (3.12), (3.13) at time t_{n+1} , we will proceed similarly as for the Galerkin discretization in Section 3. Thus, given approximations \mathbf{u}_{k-1}^{n+1} , \mathbf{c}_{k-1}^{n+1} , \mathbf{p}_{k-1}^{n+1} (with some $k > 0$) of \mathbf{u}^{n+1} , \mathbf{c}^{n+1} , \mathbf{p}^{n+1} , respectively, we compute \mathbf{c}_k^{n+1} , \mathbf{p}_k^{n+1} using (3.14), (3.15). The iterate \mathbf{u}_k^{n+1} is computed by solving the linear system

$$(\mathbb{M}_L + \theta \tau_{n+1} \mathbb{L}_{k-1}^{n+1}) \mathbf{u}_k^{n+1} = (\mathbb{M}_L - (1 - \theta) \tau_{n+1} \mathbb{L}^n) \mathbf{u}^n + \left(\sum_{j=1}^M \alpha_{ij,k-1}^{n+1} f_{ij,k-1}^{n+1} \right)_{i=1}^M, \quad (5.1)$$

where $\mathbb{L}_{k-1}^{n+1} = \mathbb{A}_{k-1}^{n+1} + \mathbb{D}_{k-1}^{n+1}$ with the matrix \mathbb{A}_{k-1}^{n+1} defined in (3.17) and the artificial diffusion matrix \mathbb{D}_{k-1}^{n+1} defined by

$$d_{ij,k-1}^{n+1} = -\max\{a_{ij,k-1}^{n+1}, 0, a_{ji,k-1}^{n+1}\} \quad \text{for } i \neq j, \quad d_{ii,k-1}^{n+1} = -\sum_{j=1, j \neq i}^M d_{ij,k-1}^{n+1}. \quad (5.2)$$

The algebraic fluxes $f_{ij,k-1}^{n+1}$ are given by

$$f_{ij,k-1}^{n+1} = (-m_{ij} + \theta \tau_{n+1} d_{ij,k-1}^{n+1})(u_{j,k-1}^{n+1} - u_{i,k-1}^{n+1}) + (m_{ij} + (1 - \theta) \tau_{n+1} d_{ij}^n)(u_j^n - u_i^n) \quad (5.3)$$

and we again consider the prelimiting step

$$f_{ij,k-1}^{n+1} := 0 \quad \text{if } f_{ij,k-1}^{n+1}(\bar{u}_j - \bar{u}_i) > 0, \quad (5.4)$$

with $\bar{\mathbf{u}}$ from (4.18). The limiters $\alpha_{ij,k-1}^{n+1}$ are computed from the fluxes $f_{ij,k-1}^{n+1}$ using the Zalesak algorithm (4.23)–(4.26). The following result shows that, under suitable time step restrictions, the above-defined iterates are uniquely determined and preserve non-negativity. This is important since, in practice, the fixed-point iterations are usually terminated when a stopping criterion is met, i.e., typically before reaching the solution of the nonlinear problem (4.17), (3.12), (3.13).

Theorem 5.1. *Consider any $n \in \{0, \dots, N - 1\}$ and $k \in \mathbb{N}$ and let $\mathbf{u}^n, \mathbf{c}^n, \mathbf{p}^n \in \mathbb{R}^M$ and $\mathbf{u}_{k-1}^{n+1}, \mathbf{p}_{k-1}^{n+1} \in \mathbb{R}^M$ be arbitrary vectors satisfying $\mathbf{u}^n \geq 0$, $1 \geq \mathbf{c}^n \geq 0$, $\mathbf{p}^n \geq 0$, and $\mathbf{u}_{k-1}^{n+1} \geq 0$, $\mathbf{p}_{k-1}^{n+1} \geq 0$. Let $\mathbf{c}_k^{n+1}, \mathbf{p}_k^{n+1}$ be given by (3.14), (3.15). Let the time step τ_{n+1} satisfy the conditions*

$$(1 - \theta) \tau_{n+1} l_{ii}^n \leq m_i, \quad \theta \tau_{n+1} \left(\mu (1 - \pi_h \mathbf{u}_{k-1}^{n+1}, \phi_i) + \chi (\nabla(\pi_h \mathbf{c}_k^{n+1}), \nabla \phi_i) \right) < m_i, \quad i = 1, \dots, M. \quad (5.5)$$

Then the linear system (5.1) has a unique solution \mathbf{u}_k^{n+1} and one has $\mathbf{u}_k^{n+1} \geq 0$, $1 \geq \mathbf{c}_k^{n+1} \geq 0$, and $\mathbf{p}_k^{n+1} \geq 0$.

PROOF. The formula (3.14) immediately implies that $1 \geq \mathbf{c}_k^{n+1} \geq 0$. Since (3.15) can be written in the form (3.11) with $u_{h,\tau}$ and $c_{h,\tau}$ defined using \mathbf{u}_{k-1}^{n+1} and \mathbf{c}_k^{n+1} , respectively, at time t_{n+1} , one has $\mathbf{p}_k^{n+1} \geq 0$. Since $\mathbb{M}_L - (1 - \theta)\tau_{n+1}\mathbb{L}^n \geq 0$ according to Lemma 4.1, the solution of (4.18) satisfies $\bar{\mathbf{u}} \geq 0$. Then (4.21) implies $\tilde{\mathbf{u}} \geq 0$ for the solution of

$$\mathbb{M}_L \tilde{\mathbf{u}} = \mathbb{M}_L \bar{\mathbf{u}} + \left(\sum_{j=1}^M \alpha_{ij,k-1}^{n+1} f_{ij,k-1}^{n+1} \right)_{i=1}^M.$$

Finally, we use the fact that \mathbf{u}_k^{n+1} satisfies

$$(\mathbb{M}_L + \theta \tau_{n+1} \mathbb{L}_{k-1}^{n+1}) \mathbf{u}_k^{n+1} = \mathbb{M}_L \tilde{\mathbf{u}}. \quad (5.6)$$

It follows from the proof of Lemma 4.1 that, under the second condition in (5.5), the matrix $(\mathbb{M}_L + \theta \tau_{n+1} \mathbb{L}_{k-1}^{n+1})$ is an M-matrix and hence \mathbf{u}_k^{n+1} is uniquely determined and satisfies $\mathbf{u}_k^{n+1} \geq 0$. \square

Remark 5.2. From the physical point of view, the quantities u , c , and p should be not only non-negative but also bounded by 1 from above. We have proved that this is the case for the approximations of c . Moreover, if this would be true also for the approximations of u , the integral form (3.9) would provide this property also for the approximations of p . Unfortunately, a proof of the upper bound for the approximations of u is not available and numerical results suggest that this bound can be violated. Note that a standard proof of upper bounds for FCT discretizations relies on the decomposition (4.18)–(4.20). Then, in particular, one would need that the solution of (4.18) satisfies $\bar{\mathbf{u}} \leq 1$ if $\mathbf{u}^n \leq 1$. Choosing $\mathbf{u}^n = \mathbf{1}$ (a vector with all components equal to 1), this requirement implies that $(1 - \theta) \mathbb{A}^n \mathbf{1} = (1 - \theta) \mathbb{L}^n \mathbf{1} \geq 0$, i.e., the row sums of the matrix $(1 - \theta) \mathbb{A}^n$ have to be non-negative. Similarly, to derive an upper bound from (5.6), one would need that $\theta \mathbb{A}_{k-1}^{n+1} \mathbf{1} \geq 0$. It is clear that the validity of these row sum conditions cannot be expected.

Remark 5.3. The second condition on τ_{n+1} in (5.5) depends on \mathbf{c}_k^{n+1} which itself depends on τ_{n+1} . Consequently, in general, one has to proceed iteratively to find τ_{n+1} which satisfies (5.5). To avoid this and also the dependence of τ_{n+1} on the fixed-point iteration index k , it is possible to replace (5.5) by (4.5), cf. Remark 4.3.

We summarize the procedure for obtaining a high-resolution positivity preserving scheme for solving (2.1)–(2.5) in Algorithm 5.1.

6 Numerical results

In the following, we present several numerical experiments to verify the positivity preserving properties of the proposed scheme for the model (2.1)–(2.5).

The computations are performed on a square domain $\Omega = (0, 20)^2$ which is decomposed into quadrilateral mesh cells obtained by uniform refinements. Precisely, after r refinements, the triangulation \mathcal{T}_h consists of 2^{2r} equal squares. If not otherwise stated, we consider five refinements, i.e., \mathcal{T}_h consists of 32×32 mesh cells. As explained above, conforming bilinear finite elements are used for approximating all unknown variables. The final time is $T = 50$ and the parameter $\epsilon = 0.2$ is used. The values of the remaining parameters of the model will be specified for the particular computations. The initial conditions are defined by

$$u^0(x) = e^{-|x|^2}, \quad c^0(x) = 1 - \frac{1}{2} e^{-|x|^2}, \quad p^0(x) = \frac{1}{2} e^{-|x|^2}.$$

If not otherwise stated, we apply the A-stable Crank-Nicolson method corresponding to $\theta = 0.5$ for the time discretization. In one case, we will also discuss the application of the unconditionally stable backward Euler

Algorithm 5.1 Iterative scheme for computing an approximation of the solution to the nonlinear FCT discretization.

```

1: Choose a tolerance Tol > 0 and a damping factor  $\beta \in (0, 1]$ .
2: Compute the initial values  $\mathbf{c}^0$ ,  $\mathbf{p}^0$ , and  $\mathbf{u}^0$  by (3.5).
3: Compute the mass matrix  $\mathbb{M}$  and the lumped mass matrix  $\mathbb{M}_L$ .
4: for  $n = 0, 1, \dots, N - 1$  do
5:   Compute the stiffness matrix  $\mathbb{A}^n$  and the artificial diffusion matrix  $\mathbb{D}^n$  and set  $\mathbb{L}^n = \mathbb{A}^n + \mathbb{D}^n$ .
6:   Choose  $\tau_{n+1}$  satisfying (4.5).
7:   Compute the intermediate solution  $\bar{\mathbf{u}}$  from (4.18).
8:   Set  $\mathbf{c}_0^{n+1} = \mathbf{c}^n$ ,  $\mathbf{p}_0^{n+1} = \mathbf{p}^n$ , and  $\mathbf{u}_0^{n+1} = \mathbf{u}^n$ .
9:   for  $k = 1, 2, \dots$  do
10:    Compute  $\mathbf{c}_k^{n+1}$  from (3.14) using  $\mathbf{c}^n$ ,  $\mathbf{p}^n$  and  $\mathbf{p}_{k-1}^{n+1}$ .
11:    Compute  $\mathbf{p}_k^{n+1}$  from (3.15) using  $\mathbf{p}^n$ ,  $\mathbf{c}^n$ ,  $\mathbf{u}^n$ ,  $\mathbf{c}_k^{n+1}$ , and  $\mathbf{u}_{k-1}^{n+1}$ .
12:    Compute the stiffness  $\mathbb{A}_{k-1}^{n+1}$  from (3.17) using  $\mathbf{c}_k^{n+1}$  and  $\mathbf{u}_{k-1}^{n+1}$ .
13:    Compute the artificial diffusion matrix  $\mathbb{D}_{k-1}^{n+1}$  from (5.2) and set  $\mathbb{L}_{k-1}^{n+1} = \mathbb{A}_{k-1}^{n+1} + \mathbb{D}_{k-1}^{n+1}$ .
14:    Compute the algebraic fluxes  $f_{ij,k-1}^{n+1}$  from (5.3) and (5.4).
15:    Compute the limiters  $\alpha_{ij,k-1}^{n+1}$  by the Zalesak algorithm (4.23)–(4.26) using the fluxes  $f_{ij,k-1}^{n+1}$  and the intermediate solution  $\bar{\mathbf{u}}$ .
16:    Compute  $\mathbf{u}_k^{n+1}$  by solving the linear system (5.1).
17:    if  $\max \{ \|\mathbf{c}_k^{n+1} - \mathbf{c}_{k-1}^{n+1}\|_M, \|\mathbf{p}_k^{n+1} - \mathbf{p}_{k-1}^{n+1}\|_M, \|\mathbf{u}_k^{n+1} - \mathbf{u}_{k-1}^{n+1}\|_M \} < \text{Tol}$  then
18:      Go to line 23.
19:    else
20:      Set  $\mathbf{c}_k^{n+1} := \beta \mathbf{c}_k^{n+1} + (1-\beta) \mathbf{c}_{k-1}^{n+1}$ ,  $\mathbf{p}_k^{n+1} := \beta \mathbf{p}_k^{n+1} + (1-\beta) \mathbf{p}_{k-1}^{n+1}$ ,  $\mathbf{u}_k^{n+1} := \beta \mathbf{u}_k^{n+1} + (1-\beta) \mathbf{u}_{k-1}^{n+1}$ .
21:    end if
22:  end for
23:  Set  $\mathbf{c}^{n+1} = \mathbf{c}_k^{n+1}$ ,  $\mathbf{p}^{n+1} = \mathbf{p}_k^{n+1}$ ,  $\mathbf{u}^{n+1} = \mathbf{u}_k^{n+1}$ .
24: end for

```

method corresponding to $\theta = 1$. Algorithm 5.1 is used with the tolerance Tol = 10^{-8} and the damping factor $\beta = 0.5$. The linear system (5.1) is solved using the sparse direct solver UMFPACK [17]. Our newly developed algorithms are implemented in the open-source finite element library deal.II [4, 5].

6.1 Comparison between the standard Galerkin FEM and the FEM-FCT scheme in presence of diffusion

To begin with, in the first example we consider the modified model subjected to an extra diffusion term in the equation (2.1) with diffusion coefficient α^{-1} , as considered in [21], i.e., the equation (2.1) is replaced by (2.6). We consider $\alpha = 10$, $\chi = 1$, and $\mu = 1$. As can be seen from Figs. 1 and 3, the FEM-FCT scheme introduces slightly more artificial diffusion than the standard Galerkin FEM. One can observe that the cancer cells invade the extracellular matrix and occupy the whole domain completely at the final time. Next, we decrease the amount of the diffusion by setting $\alpha = 1000$ and keep the proliferation and haptotaxis rate as before. As can be seen from Figs. 5 and 6, the standard Galerkin FEM shows some oscillations in the front layer and the numerical simulation breaks down when the solution reaches the boundary of the computational domain, whereas applying the FEM-FCT removes the oscillations and keeps the solution positive at all times. The corresponding snapshots of the cancer cell density, extracellular matrix, and protease are plotted along the line $y = x$ in Figs. 2, 4, 6, and 8.

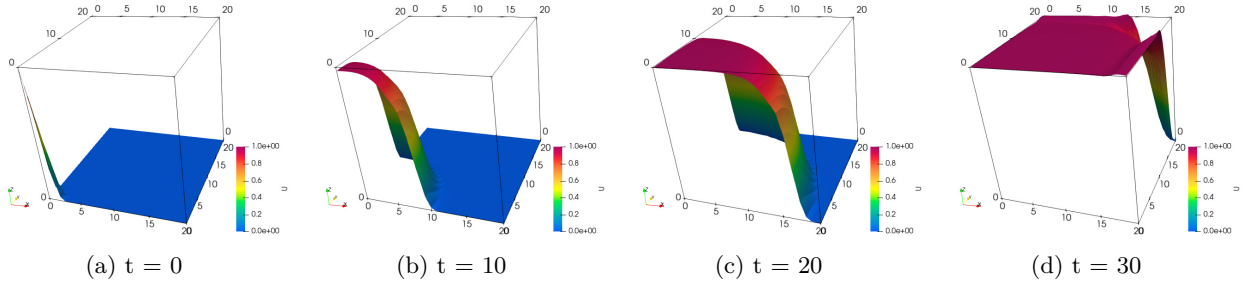


Figure 1: Cancer cell invasion u at different time instants $t = 0, 10, 20, 30$, obtained with the standard Galerkin FEM for $\alpha = 10$, $\mu = 1$ and $\chi = 1$.

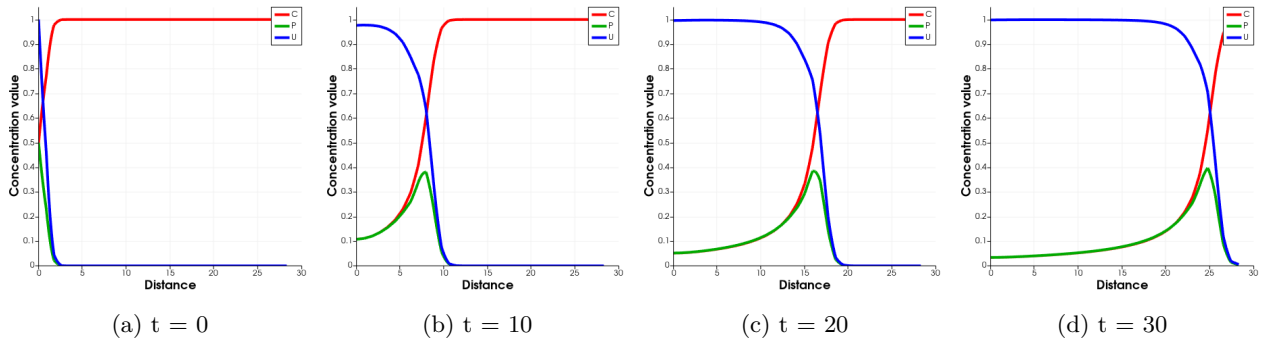


Figure 2: Cancer cell invasion u , connective tissue c , and protease p at different time instants $t = 0, 10, 20, 30$, obtained with the standard Galerkin FEM for $\alpha = 10$, $\mu = 1$ and $\chi = 1$.

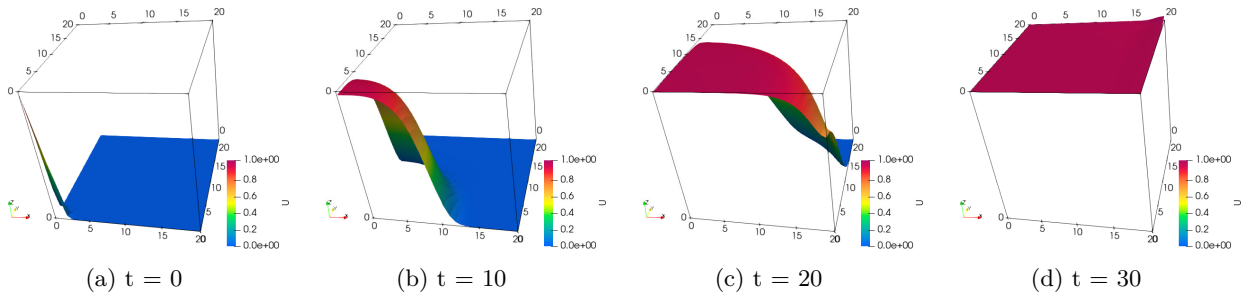


Figure 3: Cancer cell invasion u at different time instants $t = 0, 10, 20, 30$, obtained with the FEM-FCT scheme for $\alpha = 10$, $\mu = 1$ and $\chi = 1$.

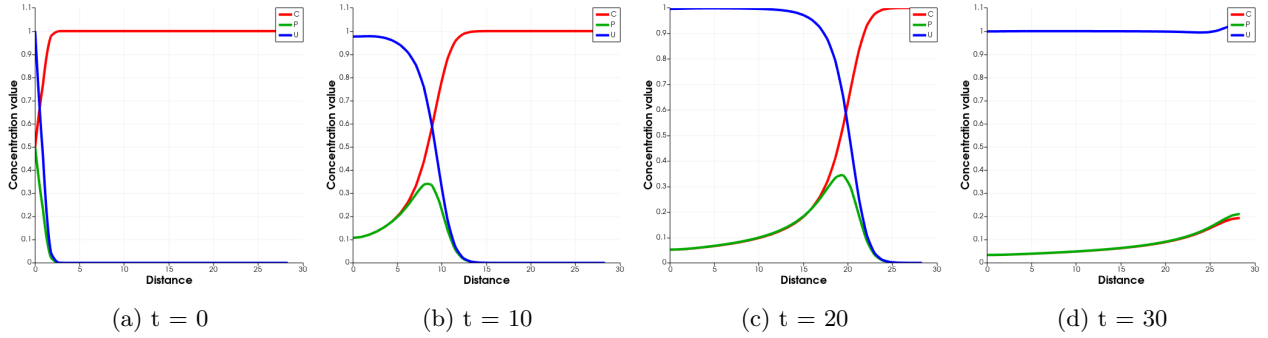


Figure 4: Cancer cell invasion u , connective tissue c , and protease p at different time instants $t = 0, 10, 20, 30$, obtained with the FEM-FCT scheme for $\alpha = 10$, $\mu = 1$ and $\chi = 1$.

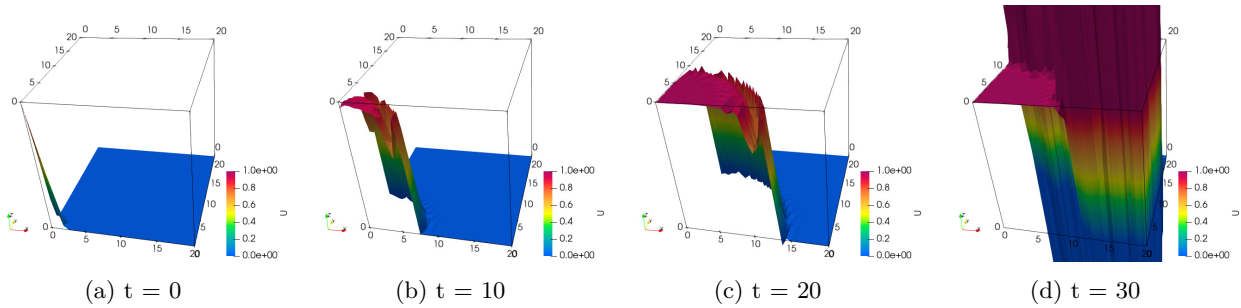


Figure 5: Cancer cell invasion u at different time instants $t = 0, 10, 20, 30$, obtained with the standard Galerkin FEM for $\alpha = 1000$, $\mu = 1$ and $\chi = 1$.

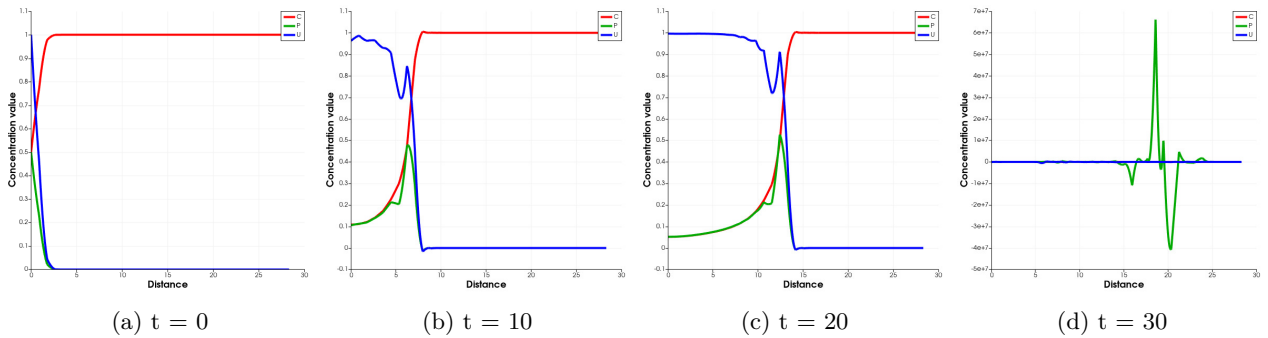


Figure 6: Cancer cell invasion u , connective tissue c , and protease p at different time instants $t = 0, 10, 20, 30$, obtained with the standard Galerkin FEM for $\alpha = 1000$, $\mu = 1$ and $\chi = 1$.

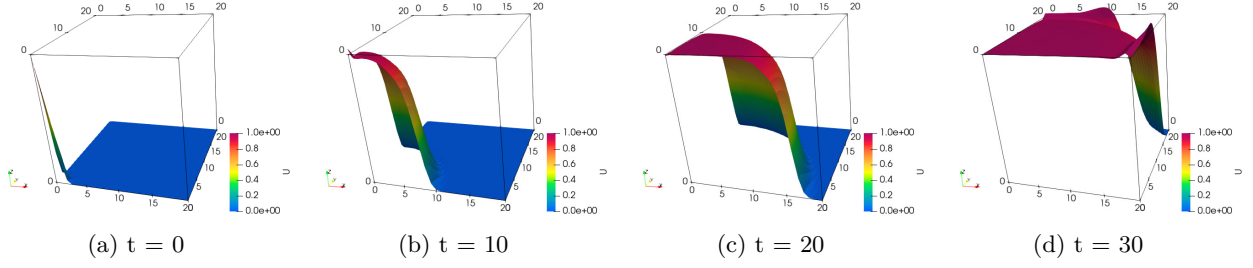


Figure 7: Cancer cell invasion u at different time instants $t = 0, 10, 20, 30$, obtained with the FEM-FCT scheme for $\alpha = 1000$, $\mu = 1$ and $\chi = 1$.

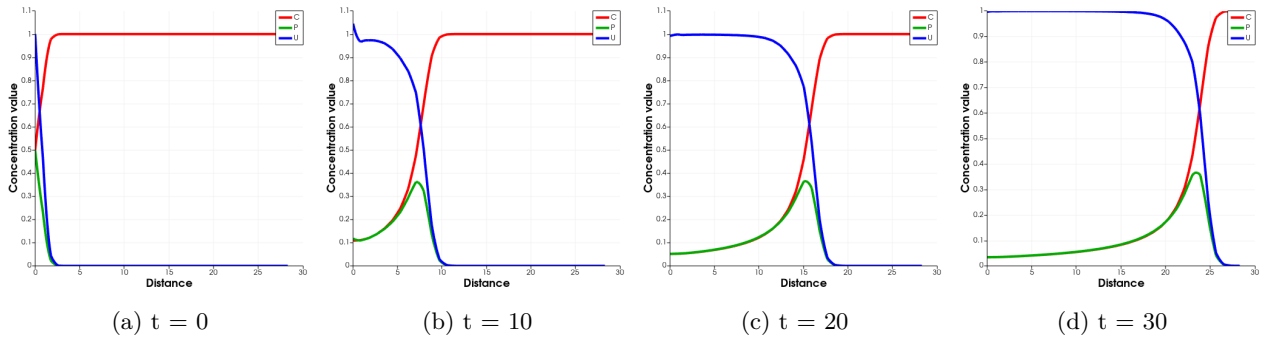


Figure 8: Cancer cell invasion u , connective tissue c , and protease p at different time instants $t = 0, 10, 20, 30$, obtained with the FEM-FCT scheme for $\alpha = 1000$, $\mu = 1$ and $\chi = 1$.

6.2 The FEM-FCT scheme in absence of diffusion for $\chi = 1$, $\mu = 1$

In this section, we consider the case without the diffusion term, i.e., utilizing (2.1) now, and again set $\chi = \mu = 1$. This case was studied in [14, 30], where the authors applied a nonstandard finite difference (NSFD) scheme using Mickens rules. The proposed methods were successful in comparison to standard finite difference methods at obtaining positive solutions, however, some wiggles still remained in the vicinity of the front layer. On the other hand, deriving an efficient NSFD scheme heavily depends on the type of the system and the discretization of different terms. Therefore, in this work, we applied the FEM-FCT methodology to remove the oscillations in the front layer while keeping the solutions positive at all times, see Figs. 9 and 10. Next, we check numerically whether the approximate solutions converge. To this end, we computed the integrals of the solutions at the final time $t = 50$ for different numbers of global refinements, see Table 1. The results correspond to the situation where the tumor is completely malignant and invades the whole extracellular matrix. In Table 2, we study the values of the solutions at the point $(20, 20)$, the differences between two consecutive iterative solutions, and the numbers of fixed-point iterations for different time steps. In particular, we observe that the proposed scheme is convergent with respect to the time step size. The convergence of the cancer cell invasion u with respect to the time step and the mesh width at two different time instants is also studied in Fig. 11 by means of solution graphs along the line $y = x$.

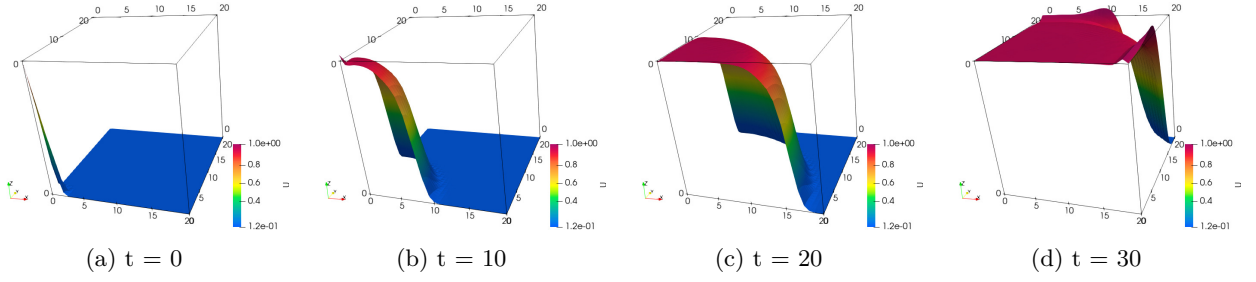


Figure 9: Cancer cell invasion u at different time instants $t = 0, 10, 20, 30$, obtained with the FEM-FCT scheme for $\mu = 1$ and $\chi = 1$.

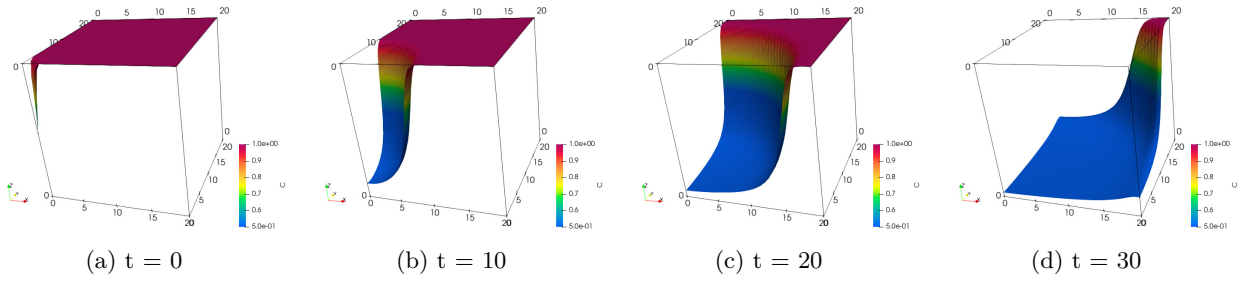


Figure 10: Decay of the extracellular matrix c at different time instants $t = 0, 10, 20, 30$, computed using the FEM-FCT scheme for $\mu = 1$ and $\chi = 1$.

Table 1: Convergence of the mean values with respect to global mesh refinement at the last time instant $t = 50$.

# of refinements	3	4	5	6	7
# DOF	81	289	1089	4225	16641
$\int_{\Omega} c_h(x) dx$	0.02362193	0.02670467	0.03284535	0.03042843	0.03680451
$\int_{\Omega} p_h(x) dx$	0.02373726	0.02685417	0.03308441	0.03062835	0.03712137
$\int_{\Omega} u_h(x) dx$	0.99999999	0.99999998	0.99999976	0.99999943	0.99999889

Table 2: Convergence of the solutions at the point $(20, 20)$ with respect to the time step τ and convergence of the fixed-point iterations, both at the last time instant $t = 50$.

τ	c_k^{n+1}	$\ c_k^{n+1} - c_{k-1}^{n+1}\ $	p_k^{n+1}	$\ p_k^{n+1} - p_{k-1}^{n+1}\ $	u_k^{n+1}	$\ u_k^{n+1} - u_{k-1}^{n+1}\ $	# Iterations
1.0	0.0333129	4.6407721e-09	0.0335600	5.0321162e-09	1.0004557	6.9181459e-11	21
0.1	0.0388396	5.5772037e-09	0.0391805	5.7753161e-09	1.0007926	4.4710309e-11	18
0.01	0.0387508	9.0822211e-09	0.0390900	9.2197598e-09	1.0007004	1.4400819e-10	14
0.001	0.0387514	7.2775629e-09	0.0390907	7.3738174e-09	1.0007904	1.2164834e-10	11
0.0001	0.0387516	5.8227737e-09	0.0390908	5.8989104e-09	1.0007904	9.7728734e-11	8

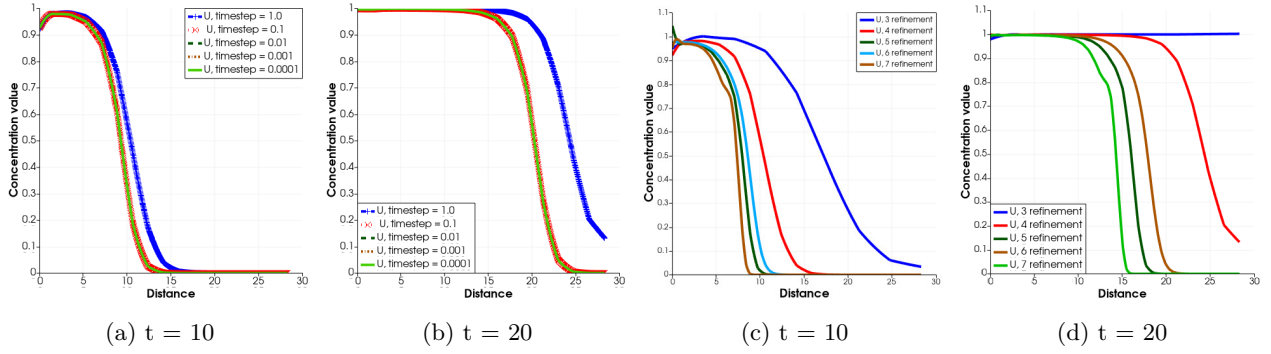


Figure 11: Cancer cell invasion u computed using the FEM-FCT scheme at time instants $t = 10$ and $t = 20$ for different time steps (first two pictures) and for different numbers of global refinements (last two pictures).

6.3 Effect of haptotactic domination

In this section, we investigate the effect of directional movement of cancer cells inside the domain. This is a very important property in cancer modeling which can lead to metastasis. In metastasis, the cancer cells are moving to the other parts of the body and start proliferate, forming a new tumor in the new part, and invade the surrounding tissues. In this case, it is very difficult to detect the location of cancerous cells and this is one of the predominant causes of most deaths due to cancer. In the following, we only study a very simple case of haptotactic dominating mechanism of the cancer cell motion. In addition to the absence of the diffusion effect in the system, there is only a small amount of the proliferation rate: we set $\mu = 0.0001$ and $\chi = 1$ in the computations. As a result of the haptotactic migration domination, a small cluster of cancer cells builds up at the beginning and this initial amount is expected to move along the direction of the gradient of the extracellular matrix. As Fig. 12 indicates, the numerical simulation by the standard Galerkin FEM breaks down in a very short amount of time after the time instant $t = 15$. Next, we apply the FEM-FCT scheme and the low-order method, see Figs. 13 and 14, respectively. We observe that, in both cases, the stabilization prevents the blow-up in the system and leads to non-negative solutions. However, some oscillations still remain in the interior layer. These oscillations could be suppressed by adaptive mesh refinement, which is however out of the scope of this paper. As expected, the low-order method provides a more diffusive solution than the FEM-FCT scheme. It is interesting that, combining the FEM-FCT scheme with the backward Euler method ($\theta = 1$), oscillation-free solutions are obtained, see Fig. 15.

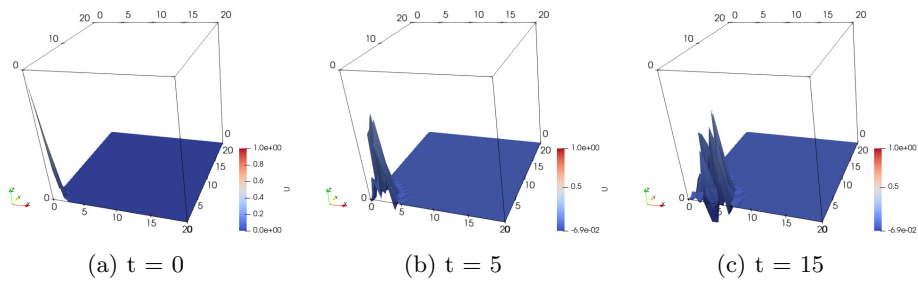


Figure 12: The effect of the haptotactic rate on the cancer cell invasion u at different time instants $t = 0, 5, 15$, computed using the standard Galerkin FEM for $\mu = 0.0001$ and $\chi = 1$.

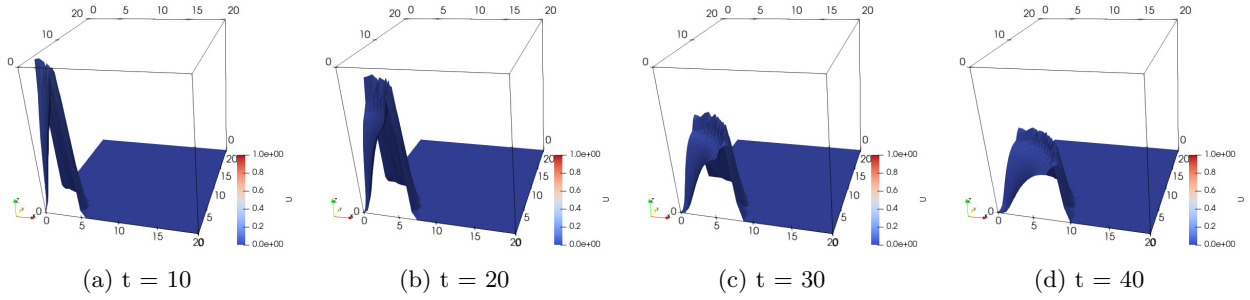


Figure 13: The effect of the haptotactic rate on the cancer cell invasion u at different time instants $t = 10, 20, 30, 40$, computed using the FEM-FCT scheme for $\mu = 0.0001$ and $\chi = 1$.

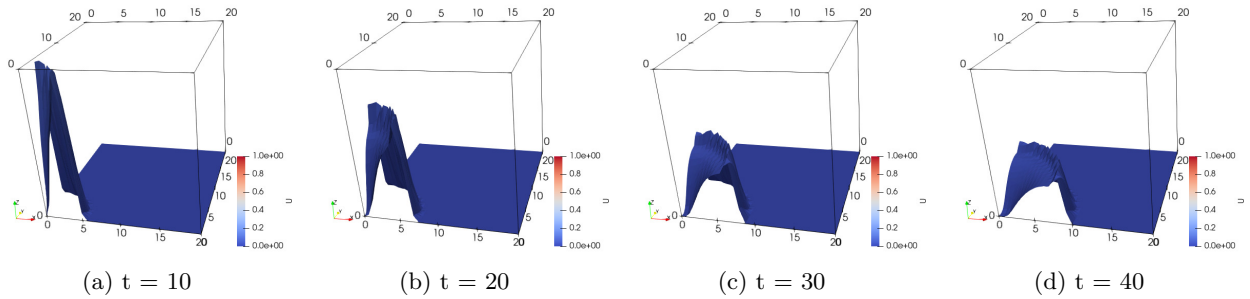


Figure 14: The effect of the haptotactic rate on the cancer cell invasion u at different time instants $t = 10, 20, 30, 40$, computed using the low-order method for $\mu = 0.0001$ and $\chi = 1$.

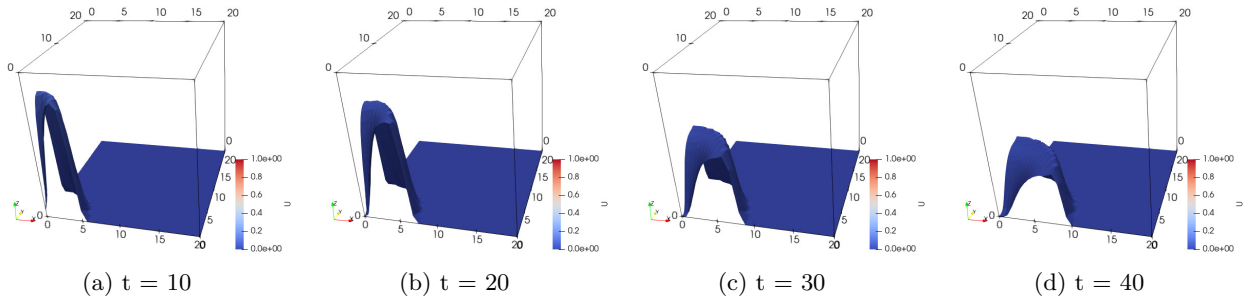


Figure 15: The effect of the haptotactic rate on the cancer cell invasion u at different time instants $t = 10, 20, 30, 40$, computed using the FEM-FCT scheme with $\theta = 1$ for $\mu = 0.0001$ and $\chi = 1$.

7 Conclusions

In this paper, we proposed a fully discrete nonlinear high-resolution positivity preserving FEM-FCT scheme for chemotaxis equations without self-diffusion term describing a model of cancer invasion. We proved the solvability and positivity preservation of both the nonlinear discrete problem and the linear problems appearing

in fixed-point iterations. A series of numerical experiments are shown to verify the robustness of the proposed method. Derivation of error estimates is left to future work.

Acknowledgments

This work was initiated during a research stay of the first author at the Institute of Applied Mathematics at the Leibniz University Hanover from November 2021 to April 2022 for which hospitality is still gratefully acknowledged. The work of Shahin Heydari was further supported through the grant No. 396921 of the Charles University Grant Agency. The work of Petr Knobloch was supported through the grant No. 22-01591S of the Czech Science Foundation.

References

- [1] Masashi Aida, Tohru Tsujikawa, Messoud Efendiev, Atsushi Yagi, and Masayasu Mimura. Lower estimate of the attractor dimension for a chemotaxis growth system. *J. London Math. Soc. (2)*, 74(2):453–474, 2006.
- [2] Masashi Aida and Atsushi Yagi. Target pattern solutions for chemotaxis-growth system. *Sci. Math. Jpn.*, 59(3):577–590, 2004.
- [3] Alexander R.A. Anderson, Mark A.J. Chaplain, E. Luke Newman, Robert J.C. Steele, and Alastair M. Thompson. Mathematical modelling of tumour invasion and metastasis. *Computational and mathematical methods in medicine*, 2(2):129–154, 2000.
- [4] Daniel Arndt, Wolfgang Bangerth, Denis Davydov, Timo Heister, Luca Heltai, Martin Kronbichler, Matthias Maier, Jean-Paul Pelteret, Bruno Turcksin, and David Wells. The DEAL.II finite element library: Design, features, and insights. *Comput. Math. Appl.*, 81:407–422, 2021.
- [5] Daniel Arndt, Wolfgang Bangerth, Marco Feder, Marc Fehling, Rene Gassmüller, Timo Heister, Luca Heltai, Martin Kronbichler, Matthias Maier, Peter Munch, Jean-Paul Pelteret, Simon Sticko, Bruno Turcksin, and David Wells. The deal.II library, Version 9.4. *J. Numer. Math.*, 30(3):231–246, 2022.
- [6] Gabriel R. Barrenechea, Volker John, and Petr Knobloch. Finite element methods respecting the discrete maximum principle for convection-diffusion equations. *SIAM Rev.*, *accepted for publication*, 2023.
- [7] D.L. Book, J.P. Boris, and K. Hain. Flux-corrected transport II: Generalizations of the method. *J. Comput. Phys.*, 18(3):248–283, 1975.
- [8] Jay P. Boris and David L. Book. Flux-corrected transport. I. SHASTA, a fluid transport algorithm that works. *J. Comput. Phys.*, 11(1):38–69, 1973.
- [9] J.P. Boris and D.L. Book. Flux-corrected transport. III. minimal-error FCT algorithms. *J. Comput. Phys.*, 20(4):397–431, 1976.
- [10] Vincent Calvez, Lucilla Corrias, and Mohamed Abderrahman Ebde. Blow-up, concentration phenomenon and global existence for the Keller–Segel model in high dimension. *Comm. Partial Differential Equations*, 37(4):561–584, 2012.
- [11] M. A. J. Chaplain and G. Lolas. Mathematical modelling of cancer cell invasion of tissue: the role of the urokinase plasminogen activation system. *Math. Models Methods Appl. Sci.*, 15(11):1685–1734, 2005.
- [12] M. A. J. Chaplain and G. Lolas. Mathematical modelling of cancer invasion of tissue: dynamic heterogeneity. *Netw. Heterog. Media*, 1(3):399–439, 2006.

- [13] Mark A.J. Chaplain and Andrew M. Stuart. A model mechanism for the chemotactic response of endothelial cells to tumour angiogenesis factor. *Mathematical Medicine and Biology: A Journal of the IMA*, 10(3):149–168, 1993.
- [14] Michael Chapwanya, Jean M.-S. Lubuma, and Ronald E. Mickens. Positivity-preserving nonstandard finite difference schemes for cross-diffusion equations in biosciences. *Comput. Math. Appl.*, 68(9):1071–1082, 2014.
- [15] P. G. Ciarlet. *The finite element method for elliptic problems*. North-Holland, Amsterdam, 1978.
- [16] L. Corrias, B. Perthame, and H. Zaag. Global solutions of some chemotaxis and angiogenesis systems in high space dimensions. *Milan J. Math.*, 72:1–28, 2004.
- [17] Timothy A. Davis. Algorithm 832: UMFPACK V4.3—an unsymmetric-pattern multifrontal method. *ACM Trans. Math. Software*, 30(2):196–199, 2004.
- [18] Yekaterina Epshteyn and Alexander Kurganov. New interior penalty discontinuous Galerkin methods for the Keller–Segel chemotaxis model. *SIAM J. Numer. Anal.*, 47(1):386–408, 2008/09.
- [19] Dianlei Feng, Insa Neuweiler, Udo Nackenhorst, and Thomas Wick. A time-space flux-corrected transport finite element formulation for solving multi-dimensional advection-diffusion-reaction equations. *J. Comput. Phys.*, 396:31–53, 2019.
- [20] Francis Filbet. A finite volume scheme for the Patlak–Keller–Segel chemotaxis model. *Numer. Math.*, 104(4):457–488, 2006.
- [21] Mario Fuest, Shahin Heydari, Petr Knobloch, Johannes Lankeit, and Thomas Wick. Global existence of classical solutions and numerical simulations of a cancer invasion model. *ESAIM Math. Model. Numer. Anal.*, 57(4):1893–1919, 2023.
- [22] Dirk Horstmann and Marcello Lucia. Uniqueness and symmetry of equilibria in a chemotaxis model. *J. Reine Angew. Math.*, 654:83–124, 2011.
- [23] Dirk Horstmann and Michael Winkler. Boundedness vs. blow-up in a chemotaxis system. *J. Differential Equations*, 215(1):52–107, 2005.
- [24] Xueling Huang, Xinlong Feng, Xufeng Xiao, and Kun Wang. Fully decoupled, linear and positivity-preserving scheme for the chemotaxis–Stokes equations. *Comput. Methods Appl. Mech. Engrg.*, 383:Paper No. 113909, 19, 2021.
- [25] Xueling Huang, Xufeng Xiao, Jianping Zhao, and Xinlong Feng. An efficient operator-splitting FEM-FCT algorithm for 3D chemotaxis models. *Engineering with Computers*, 36(4):1393–1404, 2020.
- [26] Volker John and Petr Knobloch. Existence of solutions of a finite element flux-corrected-transport scheme. *Appl. Math. Lett.*, 115:Paper No. 106932, 6, 2021.
- [27] Volker John, Petr Knobloch, and Paul Korsmeier. On the solvability of the nonlinear problems in an algebraically stabilized finite element method for evolutionary transport-dominated equations. *Math. Comp.*, 90(328):595–611, 2021.
- [28] Evelyn F. Keller and Lee A. Segel. Initiation of slime mold aggregation viewed as an instability. *Journal of theoretical biology*, 26(3):399–415, 1970.
- [29] Evelyn F. Keller and Lee A. Segel. Model for chemotaxis. *Journal of theoretical biology*, 30(2):225–234, 1971.
- [30] M. Mehdizadeh Khalsaraei, Sh. Heydari, and L. Davari Algoo. Positivity preserving nonstandard finite difference schemes applied to cancer growth model. *J. Cancer Treat. Res.*, 4(4):27–33, 2016.

- [31] Mikhail K. Kolev, Miglena N. Koleva, and Lubin G. Vulkov. An unconditional positivity-preserving difference scheme for models of cancer migration and invasion. *Mathematics*, 10(1):131, 2022.
- [32] D. Kuzmin and S. Turek. Flux correction tools for finite elements. *J. Comput. Phys.*, 175(2):525–558, 2002.
- [33] Dmitri Kuzmin. Explicit and implicit FEM-FCT algorithms with flux linearization. *J. Comput. Phys.*, 228(7):2517–2534, 2009.
- [34] Dmitri Kuzmin. Algebraic flux correction I. Scalar conservation laws. In Dmitri Kuzmin, Rainald Löhner, and Stefan Turek, editors, *Flux-corrected transport. Principles, algorithms, and applications*, pages 145–192. Springer, Dordrecht, second edition, 2012.
- [35] Xingjie Helen Li, Chi-Wang Shu, and Yang Yang. Local discontinuous Galerkin method for the Keller–Segel chemotaxis model. *J. Sci. Comput.*, 73(2-3):943–967, 2017.
- [36] Rainald Löhner, Ken Morgan, Jaime Peraire, and Mehdi Vahdati. Finite element flux-corrected transport (FEM–FCT) for the Euler and Navier–Stokes equations. *Int. J. Numer. Methods Fluids*, 7(10):1093–1109, 1987.
- [37] B. P. Marchant, J. Norbury, and A. J. Perumpanani. Travelling shock waves arising in a model of malignant invasion. *SIAM J. Appl. Math.*, 60(2):463–476, 2000.
- [38] B. P. Marchant, J. Norbury, and J. A. Sherratt. Travelling wave solutions to a haptotaxis-dominated model of malignant invasion. *Nonlinearity*, 14(6):1653–1671, 2001.
- [39] Masayasu Mimura and Tohru Tsujikawa. Aggregating pattern dynamics in a chemotaxis model including growth. *Physica A: Statistical Mechanics and its Applications*, 230(3-4):499–543, 1996.
- [40] Vidyanand Nanjundiah. Chemotaxis, signal relaying and aggregation morphology. *Journal of Theoretical Biology*, 42(1):63–105, 1973.
- [41] Abbey J. Perumpanani, Jonathan A. Sherratt, John Norbury, and Helen M. Byrne. A two parameter family of travelling waves with a singular barrier arising from the modelling of extracellular matrix mediated cellular invasion. *Phys. D*, 126(3-4):145–159, 1999.
- [42] David L. Ropp and John N. Shadid. Stability of operator splitting methods for systems with indefinite operators: advection-diffusion-reaction systems. *J. Comput. Phys.*, 228(9):3508–3516, 2009.
- [43] Norikazu Saito. Conservative upwind finite-element method for a simplified Keller–Segel system modelling chemotaxis. *IMA J. Numer. Anal.*, 27(2):332–365, 2007.
- [44] Andriy Sokolov, Ramzan Ali, and Stefan Turek. An AFC-stabilized implicit finite element method for partial differential equations on evolving-in-time surfaces. *J. Comput. Appl. Math.*, 289:101–115, 2015.
- [45] Andriy Sokolov, Robert Strehl, and Stefan Turek. Numerical simulation of chemotaxis models on stationary surfaces. *Discrete Contin. Dyn. Syst. Ser. B*, 18(10):2689–2704, 2013.
- [46] R. Strehl, A. Sokolov, D. Kuzmin, and S. Turek. A flux-corrected finite element method for chemotaxis problems. *Comput. Methods Appl. Math.*, 10(2):219–232, 2010.
- [47] Robert Strehl, Andriy Sokolov, Dmitri Kuzmin, Dirk Horstmann, and Stefan Turek. A positivity-preserving finite element method for chemotaxis problems in 3D. *J. Comput. Appl. Math.*, 239:290–303, 2013.
- [48] M. Sulman and T. Nguyen. A positivity preserving moving mesh finite element method for the Keller–Segel chemotaxis model. *J. Sci. Comput.*, 80(1):649–666, 2019.
- [49] Youshan Tao and Mingjun Wang. A combined chemotaxis-haptotaxis system: the role of logistic source. *SIAM J. Math. Anal.*, 41(4):1533–1558, 2009.

- [50] Roger Temam. *Navier-Stokes equations. Theory and numerical analysis*. North-Holland, Amsterdam, 1977.
- [51] R. Tyson, S.R. Lubkin, and James D. Murray. A minimal mechanism for bacterial pattern formation. *Proceedings of the Royal Society of London. Series B: Biological Sciences*, 266(1416):299–304, 1999.
- [52] Rebecca Tyson, L. G. Stern, and Randall J. LeVeque. Fractional step methods applied to a chemotaxis model. *J. Math. Biol.*, 41(5):455–475, 2000.
- [53] Richard S. Varga. *Matrix iterative analysis*. Springer-Verlag, Berlin, 2000.
- [54] Dianqing Wu. Signaling mechanisms for regulation of chemotaxis. *Cell research*, 15(1):52–56, 2005.
- [55] Steven T. Zalesak. Fully multidimensional flux-corrected transport algorithms for fluids. *J. Comput. Phys.*, 31(3):335–362, 1979.
- [56] Jiansong Zhang, Jiang Zhu, and Rongpei Zhang. Characteristic splitting mixed finite element analysis of Keller–Segel chemotaxis models. *Appl. Math. Comput.*, 278:33–44, 2016.
- [57] Shubo Zhao, Xufeng Xiao, Jianping Zhao, and Xinlong Feng. A Petrov–Galerkin finite element method for simulating chemotaxis models on stationary surfaces. *Comput. Math. Appl.*, 79(11):3189–3205, 2020.